XIII. SLOVENSKÁ GEOFYZIKÁLNA KONFERENCIA

11. a 12. september 2024, Bratislava

Abstrakty príspevkov

Contents

GRACE/GRACE-FO surface mass modelling by spherical and spheroidal harmonics

Michal ŠPRLÁK[1,*], Khosro GHOBADI-FAR[2], Shin-Chan HAN[3], Martin PITOŇÁK[1], Pavel NOVÁK[1]

[1] NTIS − New Technologies for the Information Society, Faculty of Applied Sciences, University of West Bohemia, Technická 8, 306 14 Plzeň, Czech Republic

[2] Department of Geosciences, Virginia Polytechnic Institute and State University, Blacksburg, Virginia, USA

[3] School of Engineering, Faculty of Engineering and Built Environment, University of Newcastle, University Drive, Callaghan, NSW 2308, Australia

Abstract: Satellite missions GRACE and GRACE-FO have mapped the time-variable gravitational (TVG) field to reveal mass redistribution within the Earth system. By approximating Earth's surface by a sphere, surface mass variations can uniquely be determined from the TVG. However, the spherical approximation is no longer tenable and some practical approaches have been proposed to accommodate the spheroidal shape of the Earth. In this study, see also *Ghobadi-Far et al. (2019)*, we develop a rigorous method for determining surface mass change on the spheroid. We derive a unique one-to-one relationship between the spheroidal spectrum of the surface mass and the spheroidal spectrum of the gravitational potential. We quantify the differences between the spherical and spheroidal approximations in a synthetic scenario and in a realistic experiment for the surface mass change rate in Antarctica and in Greenland. The improvement of TVG from GRACE and GRACE-FO necessitates spheroidal computation, particularly for quantifying mass changes in the polar regions.

Key words: sphere, spheroid, satellite missions, gravimetry, time-variable gravity, ice melting, polar regions

References

Ghobadi-Far K., Šprlák M., Han S.-C., 2019: Determination of ellipsoidal surface mass change from GRACE time-variable gravity data. Geophys. J. Int., 219, 1, 248–259, doi: 10.1093/gji/ggz292.

* corresponding author, e-mail: sprlakm@kgm.zcu.cz

A theoretical study on the spectral combination of vertical and horizontal spheroidal boundary-value problems

Martin PITOŇÁK*, Jiří BELINGER, Pavel NOVÁK, Michal ŠPRLÁK

NTIS − New Technologies for the Information Society,
Faculty of Applied Sciences, University of West Bohemia,
Technická 8, 306 14 Plzeň, Czech Republic;
e-mails: pitonakm@ntis.zcu.cz, belinger@students.zcu.cz, panovak@ntis.zcu.cz, michal.sprlak@gmail.com

Abstract: The spectral combination method involves using spectral weights, which vary with the spherical harmonic degree n, to integrate heterogeneous datasets. Originally, this technique was designed to optimally combine terrestrial gravity data with a global geopotential model to determine the geoid or quasi-geoid. Over time, it has been adapted for combining solutions to spherical geodetic boundary-value problems. Given that the Earth is significantly flattened at the poles, its shape is more akin to a rotational ellipsoid rather than a perfect sphere, a fact established by 18th-century arc measurements in South America and Lapland.

This study will apply the spectral combination method to the solutions of vertical and horizontal spheroidal boundary-value problems. We will derive the relevant spectral weights for each type of problem and their combination.

Key words: gravity field modelling, spheroidal boundary-value problem, spectral combination, spectral weights

* corresponding author, e-mail: pitonakm@ntis.zcu.cz

FarZone4IT: MatLab software for calculating far-zone effects in spherical integral transformations

Martin PITOŇÁK*, Petr TRNKA, Jiří BELINGER, Pavel NOVÁK, Michal ŠPRLÁK

NTIS − New Technologies for the Information Society,
Faculty of Applied Sciences, University of West Bohemia,
Technická 8, 306 14 Plzeň, Czech Republic;
e-mails: pitonakm@ntis.zcu.cz, trnkpe@students.zcu.cz,
belinger@students.zcu.cz, panovak@ntis.zcu.cz, michal.sprlak@gmail.com

Abstract: Integral transformations are a useful mathematical apparatus for modelling the gravitational field. They represent the mathematical basis for formulating integral estimators of gravitational field values, including error propagation. The theoretical and practical aspects of integral transformations traditionally used for calculating geoid/quasi-geoid heights in geodesy, such as Stokes's and Hotine's integral transformations, have already been studied. However, theoretical and practical concepts regarding other integral transformations, including non-isotropic (azimuth-dependent) transformations, have yet to be explored. One of the basic assumptions of integral transformations is the global data coverage. However, the availability of ground measurements is frequently limited. In practice, the global integral is divided into two complementary regions: the near- and far–zones. Non–negligible systematic effects of data in the far-zone require accurate evaluation. For this purpose, a new software library is developed in the MATLAB environment to calculate far–zone effects for integral transformations for gravitational potential gradients up to the third order. The library contains scripts for calculating integral kernels, error kernels, truncation error coefficients, and far-zone effects for a selected set of input parameters. This contribution deals with the implementation of equations defining far-zone effects and the subsequent numerical testing of the library functionality. Closed-loop tests were carried out using gravitational potential functionals generated from a global Earth's gravitational field model to check the numerical correctness of the software library. The source code of Far-

* corresponding author, e-mail: pitonakm@ntis.zcu.cz

Zone4IT is publicly available on the following link `https://gitlab.com/integral_transformation/FarZone4IT.git`.

Key words: far-zone effect, gravity field modelling, integral transformations, truncation errors

Theoretical and numerical aspects of global gravitational field modelling for spheroidal planetary bodies

Jiří BELINGER*, Veronika DOHNALOVÁ, Martin PITOŇÁK, Pavel NOVÁK, Michal ŠPRLÁK

NTIS − New Technologies for the Information Society,
Faculty of Applied Sciences, University of West Bohemia,
Technická 8, 306 14 Plzeň, Czech Republic

Abstract: The standard theoretical framework for the gravitational field determination often relies on spherical approximation. However, Earth's shape is much closer to a rotational ellipsoid flattened at the poles, as proved by the legendary expeditions of the French Academy of Sciences to South America and Lapland already in the 18th century. Contemporary investigations of solar system planetary bodies have revealed that many resemble prolate or oblate ellipsoids, whereas a high amount of them is flattened more significantly than the Earth. Four such spheroidal bodies have recently been subject to immense research interest: 1) Mars being explored by satellite and lander missions as it represents a potential target for future colonisation, 2) the asteroid Bennu explored by the sample-return satellite mission OSIRIS-REx, 3) the dwarf planet Ceres, and 4) the asteroid Vesta, both explored by the satellite mission Dawn. Moreover, several comets and asteroids with spheroidal (ellipsoidal) shapes have been subjected to intense small-body research. Consequently, there is an urgent need to formulate a modern theoretical framework for the gravitational field determination.

In this contribution, we formulate a mathematical theory for gravitational fields generated by ellipsoidal bodies. Four quantities are parametrised by a set of ellipsoidal harmonic functions inside the minimum Brillouin ellipsoid: 1) the gravitational potential, 2) the components of the gravitational gradient, 3) the components of the second order gravitational tensor, and 4) the components of the third order gravitational tensor. The internal part of these expansions is represented by multiplications of the Legendre functions of the first kind with spherical harmonics. The external part is formed by the products of the Legendre

* corresponding author, e-mail: belinger@ntis.zcu.cz

functions of the second kind with spherical harmonics. The applicability of the presented formulas is examined in numerical experiments. In particular, we systematically investigate selected numerical aspects of the Legendre functions of the first and second kind.

Key words: gravity field modelling, boundary value problems, integral transformations, ellipsoidal harmonic synthesis

3D geophysical-petrological model of the continental lithosphere in the Novohrad-Gemer region (northern Pannonian Basin, SK-HU)

Jaroslava PÁNISOVÁ[1,*], Miroslav BIELIK[1,2], Monika HURAIOVÁ [3], Dominika GODOVÁ[4], Vladimír BEZÁK[1], Patrik KONEČNÝ[5], Vratislav HURAI[1]

[1] Earth Science Institute, Slovak Academy of Sciences, Dúbravská cesta 9, 840 05 Bratislava, Slovakia

[2] Department of Engineering Geology, Hydrology and Applied Geophysics, Faculty of Natural Sciences, Comenius University, Ilkovičova 6, 842 15 Bratislava, Slovakia

[3] Department of Mineralogy, Petrology and Economic Geology, Faculty of Natural Sciences, Comenius University, Ilkovičova 6, 842 15 Bratislava, Slovakia

[4] Institute of Geophysics, Czech Academy of Sciences, Boční II/ 1401, 141 00 Prague 4 - Spořilov, Czech Republic

[5] Department of Special Laboratories, State Geological Institute of Dionýz Štúr, Mlynská dolina 1, 817 04 Bratislava, Slovakia

Abstract: Percolation of fluids and melts in the crust and the lithospheric mantle produces alteration zones with significantly disturbed physical properties, such as the electrical resistivity and seismic velocity. The geophysical signatures of metasomatized mantle include gravity responses as well, because the modified modal and chemical composition also triggers density changes. Here we show how the localized mantle metasomatism and the local anomalous gravity field can be mapped in the intraplate continental settings and interpreted using a three-dimensional integrated modelling, involving intra-crustal structures, deep faults and various upper mantle lithologies. The 3D interpretation performed using an IGMAS+ software (*Schmidt et al. 2020; Anikiev et al. 2023*) enables the integration of independent geo-datasets. The Novohrad-Gemer region (southern Slovakia/northern Hungary) is situated at the contact of the Pannonian back-arc basin with the Alpine-Carpathian Mountain arc. Studied alkali basalt

[*] corresponding author, e-mail: geofjapa@savba.sk

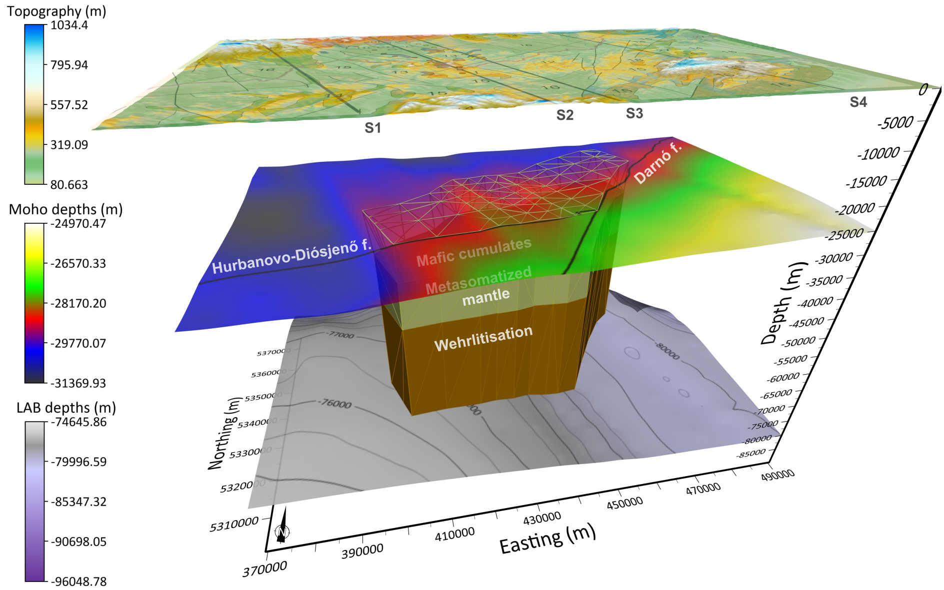

Fig. 1. Assumed structure of the anomalous segment of the Novohrad-Gemer layered mantle based on geophysical data.

volcanic field was formed during thermal subsidence of former extensional basin. Mantle xenoliths and megacrysts found here offer an excellent opportunity to study the nature and evolution of underlying lithospheric mantle. The densities of near-surface (<5 km) bodies have been defined using laboratory measurements of surface and borehole rock samples and from well-logging. To calculate rock densities at depths > 5 km, seismic V_p velocities in situ have been transformed to in situ densities ρ, while the densities of the lower lithosphere have been determined using thermodynamic modelling constrained by the chemical composition of xenoliths brought to the surface by intra-plate basalts. Thermobarometric data on megacrysts helped in constraining the vertical extent of the mantle metasomatism. Based on the proposed 3D lithospheric model of the Novohrad-Gemer region displayed in Fig. 1, the following conclusions can be drawn: a) the thickness of Neogene volcanics and sediments is variable and varies in the interval from 0 to 4 km; b) the Hurbanovo-Diósjenő-Darnó fault zone represents a steep and deeply penetrating tectonic zone, which is located beneath the central part of the Novohrad-Gemer region. North of the fault zone, the basement is built by Tatric, Veporic, and Gemeric tectonic units, which clearly show nappe structure and are included in the Alpine-West Carpathian tectonic system. South of the Hurbanovo-Diósjenő-Darnó fault zone, the basement is composed of the Northern Pannonian domain, the Transdanubian Range and the Bükk units, which all belong to the Pelso tectonic system; c) a high-density Cadomian basement was identified beneath the Veporic unit to explain the existence of pronounced gravity high overlapping the high-conductivity zone revealed by magnetotelluric sounding, with its upper boundary ranging from 12 to 18 km; d) the Darnó fault zone represents a prominent gravity feature filled with low-density rocks in the upper crust; e) in comparison with the upper crust, the lower crust is more homogeneous and divided by the Hurbanovo-Diósjenő-Darnó fault system into two blocks with densities of 2.91 $g \cdot cm^{-3}$ and 2.92 $g \cdot cm^{-3}$, respectively; f) the lithospheric mantle subjacent to the study region is characterized by a layered sandwich layout consisting of three layers: 9.0–9.5 km thick upper layer of gabbroic mafic cumulates; 12.0 km thick middle layer of the metasomatized mantle; and wehrlitized mantle in a depth interval from 50 km to 77 km. The proposed interdisciplinary approach combining geophysical, thermobarometric, thermodynamic and petrological data is applicable in other continental tectonic settings.

Key words: mantle, Moho, LAB, metasomatism, gravimetry, 3D density modelling

References

Anikiev D., Götze H.-J., Plonka C., Scheck-Wenderoth M., Schmidt S., 2023: IGMAS+: Interactive Gravity and Magnetic Application System [Computer software] GFZ Data Services, doi: 10.5880/GFZ.4.5.IGMAS.V.1.3.

Schmidt S., Anikiev D., Götze H.-J., Gomez Garcia A., Gomez Dacal M. L., Meeßen C., Plonka C., Rodriguez Piceda C., Spooner C., Scheck-Wenderoth M., 2020: IGMAS+-a tool for interdisciplinary 3D potential field modelling of complex geological structures. In: EGU General Assembly Conference Abstracts 8383.

Exploring the potential of ergodicity for regional frequency analyses of low probability rainfall extremes

Milan ONDERKA[1,2,*], Marcel GARAJ [2], Jozef PECHO[2,3], Pavel ŠŤASTNÝ[2]

[1] Earth Sciences Institute, Slovak Academy of Sciences, Dúbravská cesta 9, Bratislava, SK–840 05, Slovak Republic

[2] Slovak Hydrometeorological Institute, Jeséniova 17, Bratislava, SK–833 15, Slovak Republic

[3] Faculty of Mathematics, Physics and Informatics, Mlynská dolina F2, Bratislava, Slovak Republic

Abstract: In statistical physics, a stochastic process is said to be ergodic if its long-term time averages converge to the ensemble mean. We explored the potential of ergodic theory to deepen our understanding of the spatial patterns of rainfall extremes. Ergodicity implies that the mean (and variance) of a rainfall series can be obtained either by observing rainfall over a long period of time at one location (a rain gauge) or by observing rainfall at multiple locations over a short period of time. Assuming that a rainfall series is strictly ergodic, we can use historical data from multiple rain gauges to construct homogeneous regions and make informed decisions about water management strategies at ungauged locations. In practice, however, rainfall is measured in regions that are not homogeneous due to the involvement of various meteorological and climatological factors affecting rainfall (orographic uplifting, convergence, moisture sources, and moisture barriers, etc.). These processes are usually too complex to be modelled on a small spatial scale. Therefore, a conceptual model based on quasi-ergodicity has been proposed. The theoretical background was tested on real-world data (498 standard rain gauges and over 100 automated rain gauges and digitalized pluviographs with rainfall aggregated from 5 minutes up to 10 days. First, we focused on the spatial pattern of rainfall events with a probability of exceedance p = 10^{-2} – 10^{-3}. Precise estimates of such low-probability rainfall quantiles at ungauged locations are essential to design hydraulic infrastructure

* corresponding author, e-mail: geofmond@savba.sk

(dams, water reservoirs, drainage systems, etc.) that have to be constructed to withstand extreme rainfall amounts over time scales from a few minutes up to several days. Several data-mining techniques were tested to delineate homogeneous regions in Slovakia. Our preliminary results show that 4 homogeneous regions can be delineated for the territory of Slovakia. For each homogeneous region that fulfills the criteria of quasi-ergodicity a unique set of IDF curves has been established. Selected outcomes of out research will be presented at the Slovak Geophysical Conference 2024.

Key words: ergodicity, rainfall extremes, homogeneous region, IDF curves

Detection of subsurface cavities in Church of Saints Fabian and Sebastian in Zákupy, Czechia

Roman BERÁNEK[1,2,*], Jan MRLINA[1], Roman KŘIVÁNEK[3]

[1] Institute of Geophysics CAS,
Boční II/140 141 00 Prague 4 – Spořilov, Czech Republic

[2] Charles University in Prague,
Albertov 6, 128 43 Prague 2, Czech Republic

[3] Institute of Archaeology of the Czech Academy of Science,
Letenská 123/4, 118 00, Malá Strana, Prague 1, Czech Republic

Abstract: The members of nobility were often allowed burial in sacral buildings. Burials could be made in burial chambers or underground crypts. Such graves of privileged society are also present in the Church of St. Fabian and Sebastian in Zákupy, Czechia. The presence of two large crypts below the presbytery and sacristy is indicated by decorated tombstones with inscriptions. However, the number of possible subsurface voids/ graves in this church is substantially higher. Electromagnetic and georadar surveys revealed an unusually high number of indications of subsurface voids compared to other similar churches. To verify those findings, these methods were subsequently supplemented by a thermometry and microgravity survey. Interpret-

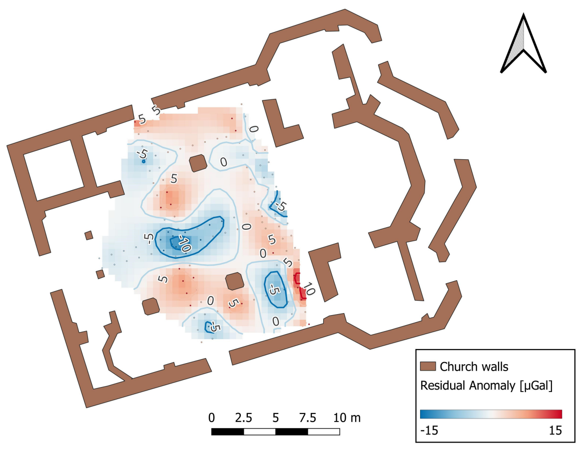

Fig. 1. Map of residual gravity anomalies in the Church of Saints Fabian and Sebastian. The source of the large negative gravity anomaly in the church nave is likely previously unknown tomb.

* corresponding author, e-mail: beranek@ig.cas.cz

ing the extensive geophysical survey led to the identification of eight zones of possible tombs or groups of graves. We have notably identified large negative gravity anomaly in the church nave (see Fig. 1), which is likely associated with a previously unknown and undocumented subsurface cavity.

Key words: near-surface geophysics, applied geophysics, crypt detection

SKTRF2022 – new national ETRS89 realization and its contribution to geokinematics of Slovakia

Martin FERIANC*, Branislav DROŠČÁK, Karol SMOLÍK

Geodetic and Cartographic Institute Bratislava,
Chlumeckého 4, 827 45 Bratislava, Slovakia

Abstract: The European Terrestrial Reference System 1989 (ETRS89) is the binding geodetic reference system in Slovakia. Until 2024, the so-called Slovak Terrestrial Reference Frame 2009 (SKTRF2009) was national realization, which corresponded to ETRF2000 at epoch 2008.5 and was defined by a set of spatial coordinates of class A and B points of the National Spatial Network (ŠPS). Within SKTRF2009, the coordinates were estimated based on the processing of continuous GNSS measurements from 2007 to 2009 at A class points of the ŠPS, i.e. permanent stations of the SKPOS network, and on previous epoch measurements at B class points of the ŠPS, i.e. points of the Slovak Geodynamic Reference Network (SGRN). Due to the short period of continuous measurements, SKTRF2009 realization did not estimate annual coordinate changes, known as velocities, which made it impossible to reliably assess geokinematics in Slovakia using GNSS measurements.

Therefore, in 2020, the Geodetic and Cartographic Institute Bratislava decided to perform a new comprehensive and homogeneous reprocessing of the entire SKPOS network of continuously operating reference permanent stations for the period from 2007 to 2020, with the aim of estimating new coordinates and velocities. The reprocessing was carried out according to the latest recommendations and standards defined by the EUREF guidelines. A total of 38 active and inactive SKPOS stations were included in the calculations. Five new SKPOS stations that had been in operation for less than three years and two stations with unstable coordinates or problematic GNSS hardware were excluded from the processing (see Fig. 1). The processing was performed with the scientific Bernese 5.2 software and included the calculation of daily coordinate solutions of the SKPOS network, which were subsequently combined to weekly solutions. The average repeatability of horizontal coordinates of individual stations was less than 1 mm, and the average repeatability of vertical coordinates was less than 2.5 mm. Subsequently, a thorough analysis of the time series of

* corresponding author, e-mail: martin.ferianc@skgeodesy.sk

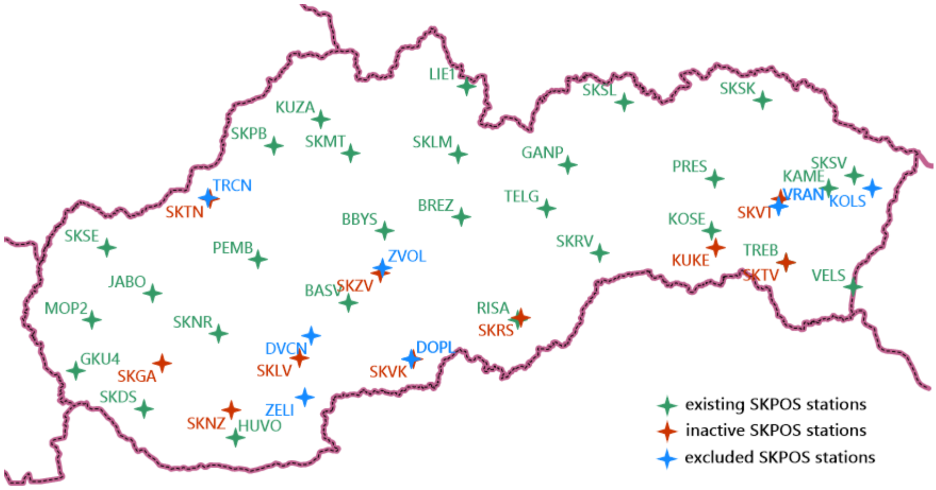

Fig. 1. Map of processed (existing/inactive) and excluded SKPOS stations.

coordinates for individual SKPOS stations was performed to identify and exclude outliers, and to estimate trends, seasonal variations, and discontinuities in the time series. Finally, the weekly SKPOS solutions were combined into a single multi-year solution, which was linked to reliable reference stations in the EUREF permanent network (EPN). The results were estimated coordinates and velocities of the SKPOS stations and residual time series of coordinates with eliminated discontinuities, trends and seasonal variations.

The accuracy of the results was assessed by comparison with three independent multi-year GNSS solutions from analysis centres within the EPN, showing very good agreement of the resulting station coordinates and velocities. In most cases, position differences did not exceed 5 mm and velocity differences did not exceed 0.50 mm/year. Based on the calculation and comparison of the estimated velocities of the SKPOS stations, we can conclude that Slovakia is located on a stable part of the Eurasian tectonic plate without significant intra-plate movements. The results did not confirm any systematic movement in a certain horizontal direction. The results indicate only a systematic subsidence of the territory of Slovakia on the sub-millimetre level. It should also be noted that the estimated velocities reach values at the level of GNSS measurement accuracy itself.

The processing results were submitted for validation to the EUREF Governing Board in 2021 and then officially accepted by resolution at the EUREF Symposium 2022 as the national realization meeting the highest quality of Class A national densification of the European reference frame. The processing results became the basis for a new national realization called Slovak Terrestrial Reference Frame 2022 (SKTRF2022), where 2022 is the year of processing. According to the amendment of Decree No. 300/2009 of the UGKK SR, SKTRF2022 became the new national realization of ETRS89 in Slovakia as of April 1, 2024.

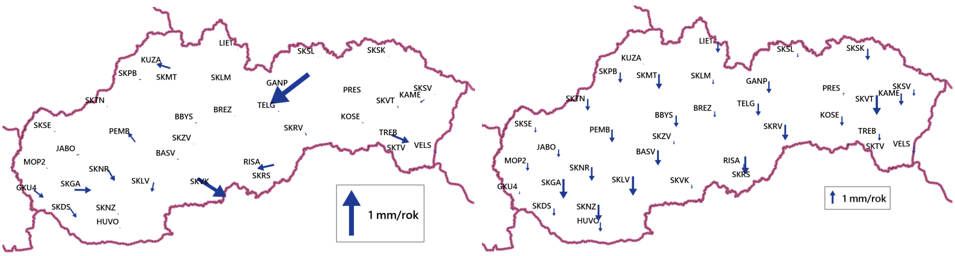

Fig. 2. Estimated horizontal (left) and vertical (right) velocities in ETRF2000.

Key words: SKPOS, GNSS, reference frame, permanent station, coordinates, velocities

Calibration of the RPSG-07 gamma radiation probe – an opportunity to celebrate the 230th anniversary of the method of least squares

Martin BEDNÁRIK[1,2,*], Andrej KOVÁČIK[1]

[1] MicroStep MIS,
Čavojského 1, 841 04 Bratislava, Slovakia

[2] Earth Science Institute SAS,
Dúbravská cesta 9, 840 05 Bratislava, Slovakia

Abstract: RPSG-07 is the newest version of the smart gamma radiation probe designed and manufactured by MicroStep MIS, a Slovakia-based company specialized in the production of measurement devices and systems for environmental monitoring. The members of the construction team were A. Kováčik, J. Hutira, J. Mačica and M. Maták.

RPSG-07 combines two Geiger–Müller tubes with different, yet overlapping measurement ranges into a single instrument with an impressive total dose rate measurement extent from 10 nSv/hour up to 10 Sv/hour. The probe counts the electric pulses triggered by the incident gamma photons in the Geiger–Müller tubes and converts their rate into the operational output quantity – the dose rate. For this transformation, the probe uses the formula:

$$y = a\,(1 - e^{-b\,x}), \qquad (1)$$

where y is the dose rate in [Sv/h], x is the pulse frequency in [count/s]=[cps]. The a parameter has the physical dimension of [Sv/h] and the b parameter [s/count]=[spc].

The calibration laboratory generates a series of accurate dose rate calibration inputs with values y_n, and the probe responds with the pulses whose rates are recorded as the calibration output series x_n. Our task is to find the parameters a and b of the function $y(x)$ (1) most closely approximating the set of input samples y_n or, alternatively, of the inverse function $x(y)$ (2) most closely approximating the output samples x_n. The user then enters the calibration parameter values a, b to the probe to ensure a precise conversion (1).

The prefered tool to solve this problem is the method of least squares (MLS) that Adrien-Marie Legendre first published in 1805 and that Carl Friedrich

* corresponding author, e-mail: geofmabe@savba.sk

Gauss claimed to have used already in 1794-5 or later, but prior to Legendre. Since the beginning of the 19th century, the claims of Gauss have been examined by various authors, with ambiguous results, cf. some relatively newer studies (*Dutka, 1996; Celmiņš, 1998*).

Many users of the MLS assume x as the independent variable whose values are correct and reliable. In our case, it is not quite true for either x or y. As for x, two gamma photons entering the gas chamber within a subcritically short time interval between them produce only one common pulse. As for y, the dose rate emitted by a reference source may decrease in time. Still, the MLS performs very well both in case of (1), and in its inverse:

$$x = -\frac{1}{b}\ln\left(1 - \frac{y}{a}\right). \tag{2}$$

If all the $[x_n, y_n]$ points cannot be fitted absolutely exactly by (1) (or (2)), then the values of a and b depend on whether the MLS is based either on (1) or (2). The question is, which of the two possibilities to prefer. Let us denote the sums of squared errors of (1) and (2) as s_{yx} and s_{xy}, respectively. As there is no obvious preference clue, a good third alternative might be a minimization of the product of the sums of squares s_{yx} and s_{xy}:

$$s = s_{yx}s_{xy}. \tag{3}$$

The differentiation with respect to a and b yields:

$$s_{,a} = \frac{\partial s}{\partial a} = s_{yx,a}s_{xy} + s_{yx}s_{xy,a}\ , \tag{4}$$

$$s_{,b} = \frac{\partial s}{\partial b} = s_{yx,b}s_{xy} + s_{yx}s_{xy,b}\ . \tag{5}$$

These expressions can be interpreted as weighted averages of the minimization criteria formulated for (1) or (2) only. As s_{yx} and s_{xy} are scaled reciprocally (because (1) and (2) are inverse functions), this weighting is just and should produce representative values of the sought parameters. We can further generalize this approach and introduce a slider parameter c running from 0 to 1 to express the weight preferences of the user:

$$r_a(c) = (1-c)s_{yx,a}s_{xy} + c\ s_{yx}s_{xy,a}\ , \tag{6}$$

$$r_b(c) = (1-c)s_{yx,b}s_{xy} + c\ s_{yx}s_{xy,b}\ , \tag{7}$$

These expressions (set equal to 0 and solved) define a continuum of least-square problems, encompassing all the three cases we refered to until now. The slider value can be either a choice of the user, or it could reflect the uncertainties of x_n and y_n.

In case of $c = 0$ or $c = 1$, we can eliminate one of the a, b parameters and reduce the two-dimensional least square problem to a nonlinear equation of the remaining parameter. The equation can be solved by many of the one-dimensional root search methods of user's convenience. We propose the interval halving or the successive linear extrapolations.

For any other value of c, the least square problem remains two-dimensional and nonlinear in both a and b. More advanced root search methods are needed. Depending on the slider parameter value, both a and b change smoothly and monotonously (Fig. 1).

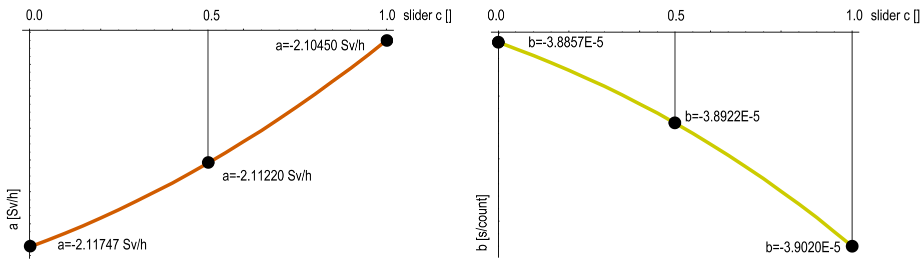

Fig. 1. Evolution of a (left) and b (right) parameter with the slider value c.

In fitting slightly inaccurate data by a parametric curve, the method of least squares is still a method of the first choice for its simplicity and robustness, even after 230 years since its first use. The numerical algorithms the MLS leads to can be (at least in our case) written from scratch and implemented even by non-programmers in the lowest-end computing environments like Microsoft Excel. Wherever appropriate, let us use and celebrate again and again the method of least squares − an everlasting meeting of mathematical elegance and practical usefulness. Cheers!

Key words: Geiger–Müller tube, calibration, method of least squares

References

Celmiņš A., 1998: The method of Gauss in 1799. Stat. Sci., **13**, 2,123–135, doi: 10.1214/ss/1028905931.

Dutka J., 1996: On Gauss' priority in the discovery of the method of least squares. Arch. Hist. Exact Sci., **49**, 355–370, doi: 10.1007/BF00374703.

Subduction zone in Northern Chile – towards an updated 3D integrated geophysical model

Dominika GODOVÁ*, Christian SIPPL

Institute of Geophysics of the Czech Academy of Sciences,
Boční II/1401, 141 00 Praha 4, Czech republic

Abstract: In the last decade, the knowledge about the geometry of the subduction zone in Northern Chile, a part of the well-studied South American active margin, has been significantly expanded thanks to seismicity data from a broad network of permanent seismic stations. That calls for incorporating new constraints in a single 3D integrated geophysical model. Since previous modelling studies mostly covered the subduction zone in larger-scale integrated models or the other parts of South America, our work aims to offer an updated view of this specific area of Northern Chile.

Our integrated geophysical modelling is based on gravity data, which bring information about different crustal density inhomogeneities and their sources. We use Complete Bouguer Anomaly computed at the Calculation Service of the International Centre for Global Earth Models (ICGEM) fromEIGEN-6C4 Global Gravity Field Model (*Foerste et al., 2014*), which includes terrestrial, satellite, and altimetry data to a high degree and order of spherical harmonic expansion. The resolution of the dataset is approximately 10 km. Since the model covers both onshore and offshore areas, topography and bathymetry data from ETOPO2022 (*NOAA, 2022*) are used.

As an inverse geophysical problem, gravity modelling is ambiguous, and therefore it is necessary to include geometry constraints from other geophysical data as well as geological information. Starting with the geometries of previously published density models in the area of the Central Andes, namely the works of *Tassara et al. (2006)* and *Tassara and Echaurren (2012)*, we modify our model according to the newest available seismicity catalogs in the study area (*Sippl et al., 2023*) together with crustal thickness values from receiver functions. Densities of modelled bodies are assigned based on previous studies.

Our contribution provides an overview of evidence compiled in previous studies and adds new information on the deep lithospheric structure of the North Chilean margin by integrating them into a single model.

* corresponding author, e-mail: dgodova@ig.cas.cz

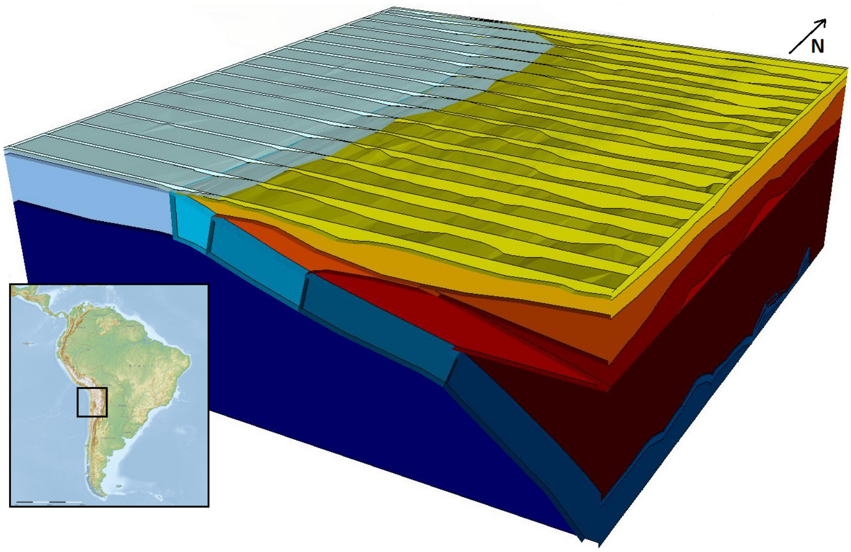

Fig. 1. 3D integrated geophysical model of the subduction zone in Northern Chile with its position within the map of South America.

Key words: mantle, Moho, LAB, metasomatism, gravimetry, 3D density modelling

References

Foerste Ch., Bruinsma S. L., Abrikosov O., Lemoin J.-M., Marty J. Ch., Flechtner F., Balmino G., Barthelmes F., Biancale R., 2014: EIGEN-6C4 The latest combined global gravity field model including GOCE data up to degree and order 2190 of GFZ Potsdam and GRGS Toulouse. GFZ Data Services, doi: 10.5880/ICGEM.2015.1.

NOAA National Centers for Environmental Information, 2022: ETOPO 2022 15 Arc-Second Global Relief Model. NOAA National Centers for Environmental Information, doi: 10.25921/fd45-gt74.

Sippl Ch., Schurr B., Muenchmeyer J., Barrientos S., Oncken O., 2023: Catalogue of Earthquake Hypocenters for Northern Chile from 2007-2021 using IPOC (plus auxiliary) seismic stations. GFZ Data Services, doi: 10.5880/GFZ.4.1.2023.004.

Tassara A., Goetze H.-J., Schmidt S., Hackney R., 2006: Three-dimensional density model of the Nazca plate and the Andean continental margin. J. Geophys. Res., **111**, B09404, doi: 10.1029/2005JB003976.

Tassara A., Echaurren A., 2012: Anatomy of the Andean subduction zone: three-dimensional density model upgraded and compared against global-scale models. Geophys. J. Int., **189**, 161−168, doi: 10.1111/j.1365-246X.2012.05397.x.

Total field measurements at the Geomagnetic Observatory Hurbanovo in the year 2023

Magdaléna VÁCZYOVÁ*

Earth Science Institute, Slovak Academy of Sciences,
Komárňanská 108, 947 01 Hurbanovo, Slovakia

Abstract: In 2006, a PMG 1 proton magnetometer was purchased for field measurements. At that time, we still had 2 proton magnetometers in operation at the observatory, ELSEC 820 and EDA. We used these devices for absolute measurements. Later, these devices broke down to such an extent that they could no longer be repaired, and we started using the PMG1 device for absolute measurements (Fig. 1.). At the same time, we also started continuous registrations of the total field in 2015.

PMG 1 is a portable device powered using an external source or from an accumulator designed to measure the total geomagnetic field by the method of the frequency of precession of protons of hydrogen nuclei.

The measurement results can be stored in the device's internal memory and transmitted via the standard RS232C serial communication channel using the PMG1tr.exe communication program [www.satisgeo.com]. In 2016, at the XVIII IAGA Workshop at the Dourbes Observatory, the accuracy of the instrument was compared with an international standard. The deviation of the device was determined to be −5.6 nT for various frequencies. Since then, the accuracy of the device has remained essentially unchanged. We compare absolute measurements during the year with the definitive values calculated from vector data.

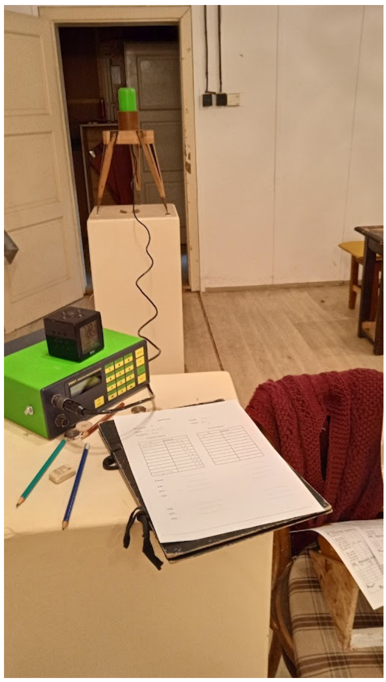

Fig. 1. Proton magnetometer PMG 1.

* corresponding author, e-mail: magdi@geomag.sk

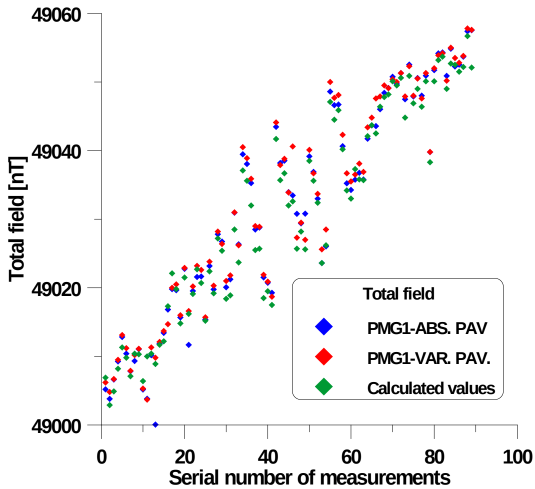

Fig. 2. Measured total field values during absolute measurements in the variation and absolute pavilion and calculated (on the base of vector registrations) definitive total field values at Hurbanovo Geomagnetic Observatory in 2023.

The disadvantage of the device is that during continuous registration, it records a lot of so-called bounced values, and these jumps are in the range of 5–600 nT.

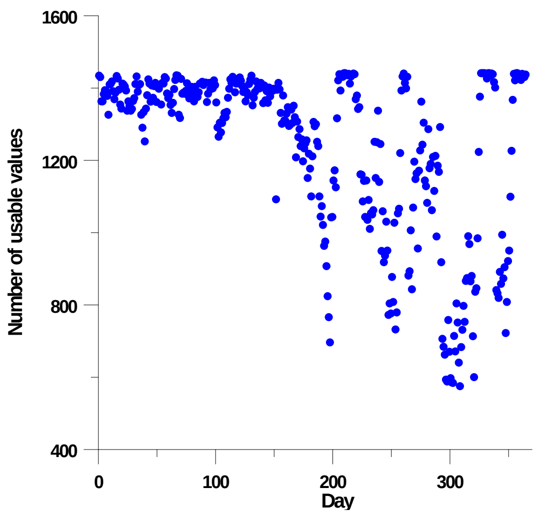

Fig. 3. Number of usable values form continous registration at the GO Hurbanovo in year 2023.

The smaller ones are difficult to remove, it is difficult to determine whether it is an artificial noise or a device error. There were days that for such reasons we had to exclude even half of the registrations per day. On average per day in 2023, the number of excluded values was 206. The number of usable total field values from continuous registration in 2023 are shown in Fig. 3. The number of bounced values turned out not to depend on the disturbances of the field.

A detailed examination of the applicability of the PMG 1 instrument as a part of the observatory practice is the subject of our paper.

Key words: total geomagnetic field, proton magnetometer, Geomagnetic Observatory Hurbanovo

The new form of regularized differentiation operator

Roland KARCOL*, Roman PAŠTEKA

Department of Engineering Geology, Hydrogeology and Applied Geophysics, Comenius University in Bratislava, Slovakia

Abstract: The evaluation of horizontal and vertical derivatives (HD or VD) is an unstable process. The possible (partial) answer to this instability is the Tikhonov regularization based on incorporating an additional (smoothing) property to the desired solution. This property is typically obtained as low-pass filter controlled by a regularization parameter (RP). Here we briefly introduce the newly obtained shape named as *General Form* (GF).

Theory

The *Classical Form* (CF, no regularization) and the *Original Form* (OF) (e.g. *Pašteka et al., 2009*) are well-known and widely used. Interesting but less-known option is the *Strakhov's Form,* SF (*Mudretsova and Veselov, 1990*).

The newly presented GF is based on the modified approach to the functional which describes the properties of the desired solution. The first functional (F_1) express the closeness of the regularized solution *f* and classical (non-regularized) solution on the grid/surface Ω:

$$F_1^{GF} = \int_{\Omega} \left[A^{-1}(f) - U_\delta \right]^2 dxdy\,,$$

where $A(\;)$ is the operator of the classical HD or VD applied on the measured field U_δ. The second (stabilizing) functional (F_2) describes the additional property of the desired solution *f* – not to be disturbed (oscillating) too much:

$$F_2^{GF} = \int_{\Omega} \left[\left(f'_x\right)^2 + \left(f'_y\right)^2 \right] dxdy\,,$$

Next, the complete functional is built up:

$$I(f) = \int_{\Omega} \left\{ \left[A^{-1}(f) - U_\delta \right]^2 + \alpha \left[\left(f'_x\right)^2 + \left(f'_y\right)^2 \right] \right\} dxdy\,,$$

* corresponding author, e-mail: roland.karcol@uniba.sk

where α is the RP and controls the “strength” of the stabilizing functional. The task – the search for the minimum of this functional, is solved by tools of variational calculus and Fourier transform:

$$\tilde{f}_x^{GF} = \frac{iu \cdot \tilde{U}_\delta}{1+\alpha \cdot iu \cdot \left(u^2+v^2\right)}, \tilde{f}_y^{GF} = \frac{iv \cdot \tilde{U}_\delta}{1+\alpha \cdot iv \cdot \left(u^2+v^2\right)}, \tilde{f}_z^{GF} = \frac{\sqrt{u^2+v^2} \cdot \tilde{U}_\delta}{1+\alpha\sqrt{u^2+v^2}\left(u^2+v^2\right)}.$$

Testing

The input field for the first synthetic test is the vertical component of the gravitational attraction vector produced by two 2D prisms (Fig. 1a) affected by 2% noise. The C norms for the newly developed GF and known OF and the solutions compared with the analytical field are placed in the Fig. 1b,c and 1d.

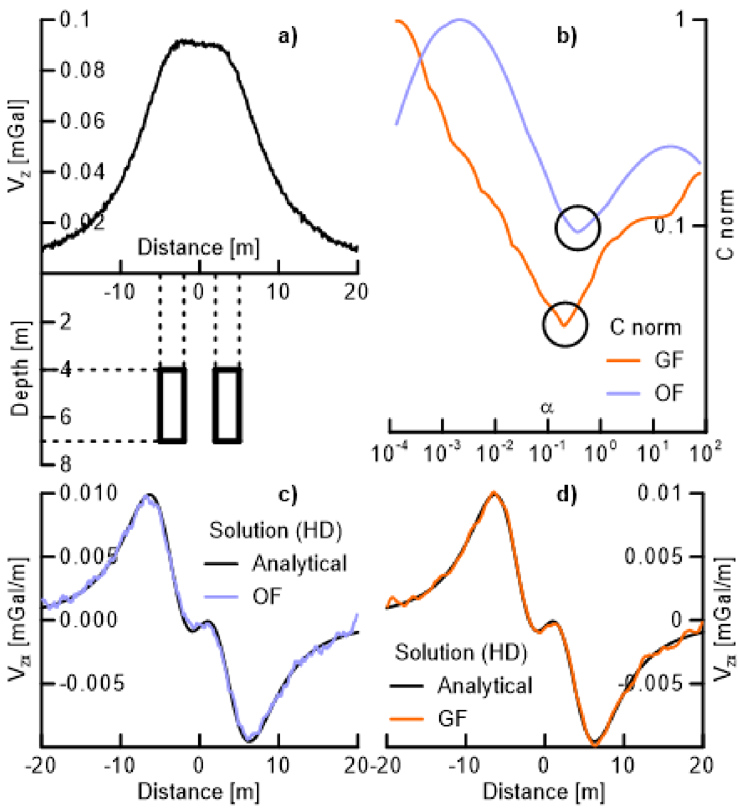

Fig. 1. The input field (a), the C norms (b) and the reg. solutions for the synthetic test (c for the OF, d for the GF).

We can see several features: the C norms contain well-developed local minima (the GF's norm is more disturbed). However, the solutions calculated for these local minima are slightly different – the OF's solution is more disturbed then GF's solution when compared to the analytical solution. Of course, one can have the OF's solution be more smooth too by increasing of the RP, but the fit with analytical solution will be weaker in the extremal values and more, the RP has to be selected by different way (e.g. another L_p norm, L curve (*Hansen, 1994*), Shape of Anomaly (*René, 1986*) a.o. or still valid trial-and-error method).

Conclusion

The several tests (where one of them and the most simple is presented here) shows that newly presented General Form of the regularized differentiation operator is worth of future testing and possible later application in the transformation of the potential field data.

Key words: potential fields, horizontal/vertical derivatives, regularization

References

Hansen P. C., 1994: Regularization Tools: A MatLab package for analysis and solution of ill-posed problems. Numer. Algorithms, **6**, 1-35, doi: 10.1007/BF02149761.

Mudretsova E. A., Veselov K. E., 1990: Gravirazvedka: Publishing House Nedra, Moscow, 608 p, (in Russian).

Pašteka R., Richter F. P., Karcol R., Brazda K., Hajach M., 2009: Regularized derivatives of potential fields and their role in semi-automated interpretation methods. Geophys. Prospect., **57**, 4, 507–516, doi: 10.1111/j.1365-2478.2008.00780.x.

René R. M., 1986: Gravity inversion using open, reject, and "shape-of-anomaly" criteria. Geophysics, **51**, 4, 988−994, doi: 10.1190/1.1442157.

Pilot geophysical survey of Newgrange Passage Tomb, Ireland

Roman PAŠTEKA[1,*], Kevin BARTON[2], Pavol ZAHOREC[3], Juraj PAPČO[4], Ema NOGOVÁ[1,3]

[1] Department of Engineering Geology, Hydrogeology and Applied Geophysics, Faculty of Natural Sciences, Comenius University, Slovak Republic

[2] Landscape and Geophysical Services, Claremorris, County Mayo, Ireland

[3] Earth Science Institute, Slovak Academy of Sciences, Banská Bystrica, Bratislava, Slovak Republic

[4] Department of Theoretical Geodesy, Faculty of Civil Engineering, Slovak University of Technology, Bratislava, Slovak Republic

Abstract: Newgrange is a Neolithic passage tomb (Fig. 1, left) in the Boyne Valley, Ireland. It was constructed about 5200 years ago and is widely known for its 19 metre-long inner passage, which leads to a cruciform chamber with a corbelled roof. The tomb is covered by a flat-topped, roughly circular mound or cairn of stones 11 m in height, averaging 82 m in diameter and covering an area of about 1 ha. A continuous kerb, comprising 97 massive stones, encircles the base of the mound (*Lynch et al., 2014*). The possibility of the existence of a second chamber in the mound has been discussed by many experts, and also non-

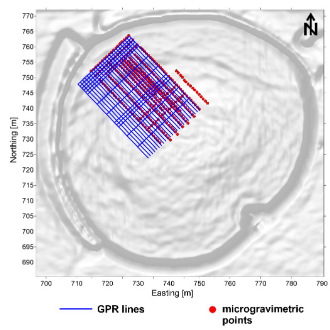

Fig. 1. Left: Newgrange mound (source: `https://www.newgrange.com/`); Right: Positions of GPR lines and microgravimetric points.

* corresponding author, e-mail: roman.pasteka@uniba.sk

specialists for many decades. As part of the narrative of the TV documentary entitled “Rún na Bóinne” (produced by IWR MEDIA) a pilot geophysical survey was conducted on the mound in a collaboration between Slovak and Irish geophysicists and geodesists (*Boyle*, *2024*).

The survey consisted of georadar (GPR) and microgravity measurements and was conducted in the northwest part of the mound (Fig. 1, right part). Using GSSI 100 MHz and 200 MHz antennas, an area of 23 metres by 35 metres was surveyed in 24 northwest to southeast lines from the rear kerb stones to the top of the cairn. The line spacing was 1 metre and sampling interval was 5 cm. In addition, 13 southwest to northeast lines were also surveyed at an irregular line spacing. With the processing parameters selected, the 100 MHz antenna achieved depths of 8 to 9 metres. The radar detected two boundaries or layers. Nearer the kerb, the detected layer is less compacted and comprises less dense material. Further into the cairn the radar detected a second, harder surface or boundary. The interpretation is that the first layer is part of the cairn, less dense but compacted material with a possible higher clay content. The harder boundary, as you extend further into the cairn, is possibly a layer with a higher rock and stone content.

At the intersection of these two boundaries, recognized in the cairn structure, the 100 MHz antenna detected two ‘anomalies’ or features (Fig. 2, top part). These are separate objects from the two identified layers, not part of them. In the data, these features appear side by side and viewed together are generally linear in shape. They were detected on all intersecting lines. Taken together they extend to a length of approx. 10–11 metres. Within this area, each has dimensions of about 3 to 4 metres in length and an average width of 1.5 metres (Fig. 2, bottom, left). Here, radar results produce weaker and poorly developed reflection waves that could be the result of a collapsed cavity or another dominant structural feature in the cairn. The antennas detected the top of these two features and not the bottom; this is normal in the case of cavities.

Two Scintrex gravity meters, models CG-5 and CG-6 were used for microgravity measurements. The microgravity survey did not detect the two features seen in the GPR results. However, it did detect a low-density zone nearer to the surface (Fig. 2, bottom, right). This zone partly overlies the location of the GPR features if their location is projected upwards to the surface. Therefore, while not detecting cavities, the microgravity data compliments the 200 MHz antenna data as both detected disturbances near the surface. The modelling of this low density zone produced a result that is consistent with a possible interpretation of a surface disturbance created by a deeper collapse. It should be noted that if there is no strong contrast in density, then the microgravity method cannot detect it.

When viewed together, both surveys partly correlate (Fig. 2, bottom, right). These results could be interpreted to indicate we are dealing with two cavities in a collapsed state. Our results are from a non-invasive remote sensing survey, the way to confirm the results would be to carry out an archaeological excavation or exploratory coring.

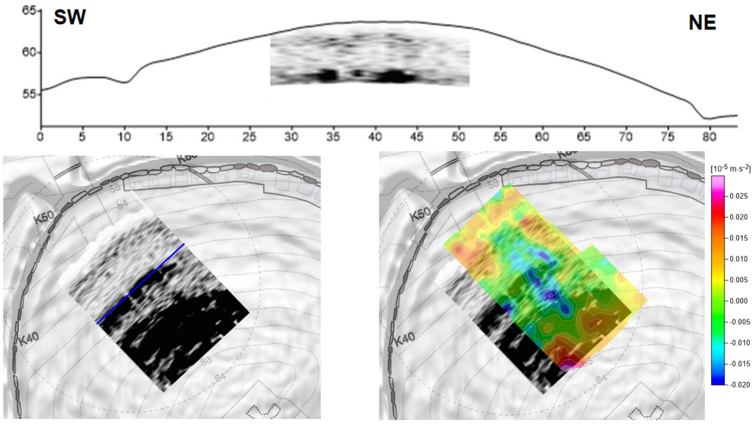

Fig. 2. GPR and microgravity results. Top: vertical GPR section showing the two adjacent interpreted features; Bottom, left: horizontal GPR slice for 7.6 m penetration depth; Bottom, right: residual Bouguer anomaly map (overlain on the horizontal GPR slice). Results in the bottom part are superimposed on a digital elevation model of the cairn with the location of pre-existing excavation cuttings (*Lynch et al., 2014*).

Key words: archaeogeophysics, georadar, microgravity, Neolithic mound

References

Boyle N., 2024: Newgrange: the second chamber. Archaeology Ireland, **38**, 147, 14–18.

Lynch A., McCormick F., Shee Twohig E., McClatchie M., Molloy K., Schulting R., O'Carroll E., Sternke F., 2014: Newgrange revisited: new insights from excavations at the back of the mound in 1984–8. J. Ir. Archaeol., **23**, 13–82.

Selected historical geomagnetic observations at the Ógyalla Observatory, now Hurbanovo

Fridrich VALACH[1,*], Magdaléna VÁCZYOVÁ[1], Eduard KOČI[1,2]

[1] Geomagnetic Observatory, Earth Science Institute, Slovak Academy of Sciences, Komárňanská 108, 947 01 Hurbanovo, Slovak Republic

[2] Slovak Central Observatory, Komárňanská 137, 947 01 Hurbanovo, Slovak Republic

Abstract: Even in the scientific community, the official date of the establishment of the Hurbanovo Geomagnetic Observatory, 30 September 1900, is often identified with the beginnings of geomagnetic observations at Hurbanovo; at that time known as Ógyalla. The fact is that officially, systematic geomagnetic observations at Ógyalla had already been performed seven years earlier (since mid-1893) (*Valach et al., 2024*). Moreover, Nicolas de Konkoly, the founder of the observatory, and Guido Schenzl had already made the first documented geomagnetic field (GMF) measurements here long before, in 1873, 1874, and 1875. Figure 1 shows the time series of annual averages (blue dots) from the very beginning of the observations at Ógyalla to the present for the three elements of the GMF, namely declination (D), inclination (I), and the horizontal component of the GMF (or horizontal intensity, H). For years 1873/1875, one common mean value (red dot) is shown for each element (*Barta, 1952*). Because long-time series of observations are very valuable in geophysics, due attention should be paid to old records. On the one hand, historical observations tended to be characterized by larger measurement uncertainties compared to modern observations, for example, because contemporary measurement devices did not allow as high measurement precision as modern ones. On the other hand, however, to study extreme phenomena such as magnetic storms, the including of historical observations is beneficial as it greatly expands the database of rarely occurring extreme events. The importance of such data is even greater when the observations are from areas sparsely covered by observatories, as was the case with the Ógyalla observatory in the 19th century. In our contribution we will present three historical magnetic storms and try to interpret them: the storms mentioned above occurred in March 1894, September 1898 and October/November 1903. All three events were accompanied by auroras observed at

[*] corresponding author, e-mail: fridrich.valach@savba.sk

mid-latitudes; this fact may help in the interpretation of the storms, as it suggests that the auroral oval was extended to geomagnetic mid-latitudes during them. Comparisons with data from other world observatories (data sources: *WDC Kyoto, 2024; Hejda et al., 2021*) have identified rapid and large local variations in the GMF during these events, the cause of which could probably be found not only in the enhanced ring current but also in the auroral oval currents and a field-aligned-current system that feeds them. Further more detailed research on historical magnetic storms may contribute to better understanding of the mechanism of these interesting phenomena. The presented research was supported by the VEGA agency with project 2/0003/24.

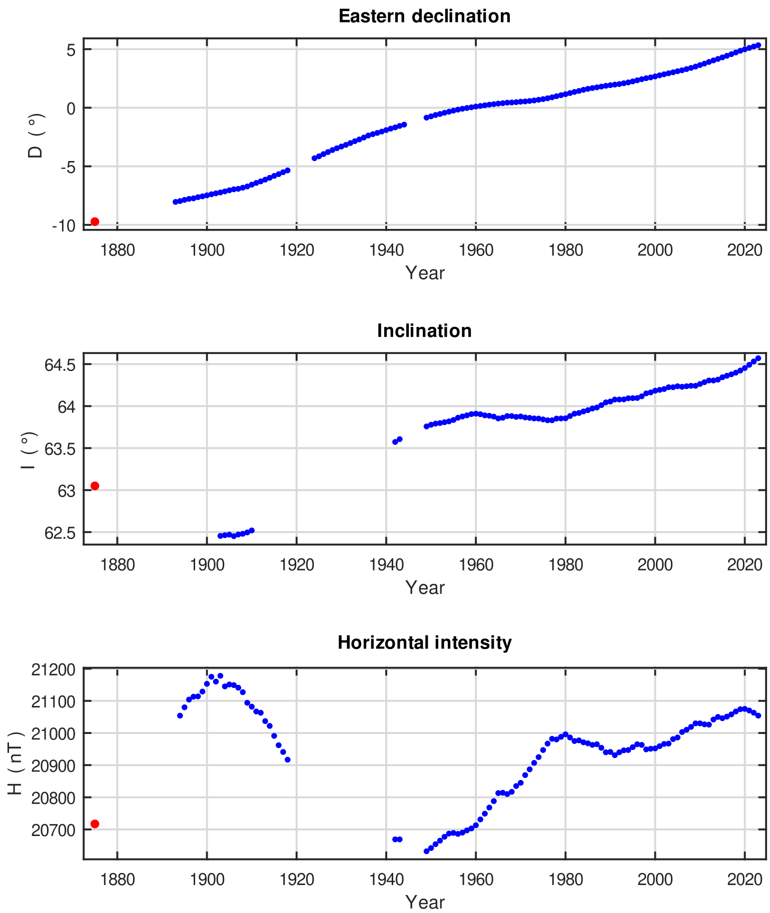

Fig. 1. Elements of the geomagnetic field observed in Ógyalla/Hurbanovo.

Key words: geomagnetic field, geomagnetic storm, extreme event

References

Valach F., Váczyová, Výberči, Koči E., 2024: Regular observations of the geomagnetic field at the Ógyalla observatory (present-day Hurbanovo) near the turn of the 20th century, including magnetic storms accompanied by auroras in March 1894, September 1898, and October 1903. Contrib. Geophys. Geod., **54**, 1, 23–48, `doi: 10.31577/congeo.2024.54.1.2`.

Barta Gy., 1952: A földmágnességi értékek változásának törvényszerűségei hazánkban. In: Magyar tudományos akadémia Műszaki tudományok osztályának Közleményei, V, 181–208 (in Hungarian).

World Data Center (WDC) for Geomagnetism Kyoto, 2024: Created and operated by Data Analysis Center for Geomagnetism and Space Magnetism, Graduate School of Science, Kyoto University, `https://wdc.kugi.kyoto-u.ac.jp/caplot/index.html`, last access: 26 August 2024.

Hejda P., Valach F., Revallo M., 2021: The geomagnetic data of the Clementinum observatory in Prague since 1839. Ann. Geophys., **39**, 439–454, supplement, `doi: 10.5194/angeo-39-439-2021`.

Geomagnetic observations at the Clementinum Observatory in Prague between 1839 and 1926

Fridrich VALACH[1,*], Pavel HEJDA[2] Miloš REVALLO[3]

[1] Geomagnetic Observatory, Earth Science Institute, Slovak Academy of Sciences, Komárňanská 108, 947 01 Hurbanovo, Slovakia

[2] Institute of Geophysics, Academy of Sciences of the Czech Republic, Boční II/1401, 14131, Prague, Czech Republic

[3] Earth Science Institute, Slovak Academy of Sciences, Dúbravská cesta 9, 840 05 Bratislava, Slovakia

Abstract: In this paper, we present selected results of our work on the digitization of geomagnetic data from the historical Prague-Clementinum Observatory. Systematic geomagnetic observations at this observatory began as early as July 1839 and were recorded in a series of yearbooks. We have converted the data into the SI system of units. In doing so, we also made the necessary corrections for the first years of observations; these consisted mainly of determining the correct temperature coefficients for the bifilar instrument, a key device for observing changes in the horizontal intensity of the geomagnetic field. We will also present two interesting intense storms observed in Prague on 3 September 1839 and 17 November 1848. These storms might be valuable for studying geomagnetic activity as part of the modern scientific discipline of space weather. The presented research was supported by the VEGA agency with project 2/0003/24.

Key words: geomagnetic observatory, geomagnetic field, geomagnetic storm

[*] corresponding author, e-mail: fridrich.valach@savba.sk

3D high-resolution numerical modelling of altimetry-derived marine gravity data

Róbert ČUNDERLÍK*, Marek MACÁK, Michal KOLLÁR, Zuzana MINARECHOVÁ, Karol MIKULA

Department of Mathematics and Descriptive Geometry, Faculty of Civil Engineering, Slovak University of Technology,
Radlinského 11, 810 05 Bratislava, Slovakia

Abstract: We present 3D numerical modelling of the altimetry-derived marine gravity data with the high horizontal resolution 1 x 1 arc min. The finite volume method (FVM) as a numerical method is used to solve the altimetry-gravimetry boundary-value problem. Large-scale parallel computations result in disturbing potential in every finite volume of the discretized 3D computational domain between an ellipsoidal approximation of the Earth's surface and upper boundary chosen at altitude of 200 km. Afterwards, the first, second or third derivatives of the disturbing potential in different directions are numerically derived using the finite differences. A process of preparing the Dirichlet boundary conditions over ocean/seas has a crucial impact on achieved accuracy. It is based on nonlinear filtering of the geopotential generated on a mean sea surface (MSS) from a GRACE/GOCE-based satellite-only global geopotential model.

We present different types of the altimetry-derived marine gravity data obtained on the DTU21_MSS as well as at higher altitudes of the 3D computational domain. The altimetry-derived gravity disturbances on the DTU21_MSS are tested by shipborne gravimetry and compared with those from the recent datasets like DTU21_GRAV or SS_v31.1. The obtained altimetry-derived gravity disturbances at higher altitudes are compared with airborne gravity data from the GRAV-D campaign in US. The gravity disturbing gradients as the second derivates or the third derivatives are provided with the same high resolution on the DTU21_MSS as well as at different altitudes.

Key words: altimetry-derived marine gravity data, high-resolution global gravity field modelling, altimetry-gravimetry boundary-value problem, finite volume method, numerical solution, large-scale parallel computations

* corresponding author, e-mail: robert.cunderlik@stuba.sk

Integrated geophysical study of tectonic dislocations in the Western Carpathians

Ján VOZÁR[1], Vladimír BEZÁK[1,*], Radek KLANICA[2], Svetlana KOVÁČIKOVÁ[2], Lenka ONDRÁŠOVÁ[1], Graham J. HILL[2]

[1] Earth Science Institute of the Slovak Academy of Sciences, Bratislava, Slovakia, e-mail: geofjavo@savba.sk

[2] Institute of Geophysics, Academy of Sciences of the Czech Republic, Czech Republic

Abstract: The tectonic structure of the Western Carpathians contains numerous tectonic units of various ages from different stages of tectonic development. These units can often be identified based on their different physical properties. To do this, it is best to use combined geophysical data from several methods.

The knowledge of geological structures and dislocation mechanisms (e.g. faults) is important when investigating a number of solid earth questions such as seismic risk, slope deformation, radon emanation and provides important information about tectonic development of the area. Co-located geophysical (magnetotelluric-MT, gravimetric, and others) and structural mapping within the Western Carpathians has lead to development of new methodology to study dislocation within the DISLOCAT project.

Integrated geophysical modelling has already yielded very good results in the past when it comes to distinguishing between tectonic units, their tectonic boundaries, and faults. Among the geophysical methods, MT provides very good results in terms of identification of faults, fracture structures and deeper suture zones based on mapping the 3D distribution of electrical conductivity, where conductive structures potentially allow fracture mapping of conductive fluids accumulated in the damaged zone in the brittle crust. Conductive minerals can also cause similar effects in fractures – typically an indication of paleo-fluids. These metallic-mineral phases precipitate from carbon rich fluids penetrate areas of shear-weakened crust, triggering chemical reactions resulting in mineralized veins and fissures.

One of the chosen areas is connected with dislocations in the Tatry Mountains and its tectonic development in the area of the European Platform and Inner

* corresponding author, e-mail: geofbezv@savba.sk

Western Carpathian junction. It resulted in an extensive shear zone, creating a corridor for the sub-vertical outflow of mantle fluids leading to formation of the deep seated Carpathian conductivity anomaly (CCA). During recent years several short MT profiles were measured to map boundaries of the Tatry Mts., which represent a crystalline complex covered by Mesozoic sedimentary rocks in the north and surrounded by a sedimentary succession of the Inner Carpathian Paleogene Basin. The preliminary conductivity and other geophysical models focus on the identification of the sub-Tatric fault and other similar discontinuities.

A second recently focus area is situated in southern Slovakia in the Gemericum unit region where the largest accumulation of ore occurs. We map mineralization zones and the Rožňava fault in the southern part of this area. The geological units and fault positions were mapped by newly collected MT data where 3D modelling with topography has been used to avoid distortion from deep valleys in the area. The MT model was coupled with the map of Bouguer anomalies and magnetic data were modelled to show correlation of studied geological features and different geophysical parameters. These results will help to understand the direction, inclination, depth and thickness of the fault zone, structural parameters and tectonic development of this area.

Key words: magnetotellurics, fault zones and dislocations, integrated geophysical modelling

Optimization of millisecond timing delay of blastings in quarries using seismic waves

Blažej PANDULA[1,*], Julián KONDELA[1], Vladimír BUDINSKÝ[1], Ján BAULOVIČ[2], Ivan BUCHLA[3]

[1] Institute of Geosciencies BERG Faculty Technical University of Košice, Slovakia

[2] SSE Slovakia

[3] Carmeuse Slovakia
Members of Slovak society for blasting and drilling works

Abstract: Blasting induced vibration is one of the fundamental problems in the quarries and intense vibration can cause critical damage to environment nearby the quarries. Blasting operations generate seismic waves with different maximum particle velocity and wide spectrum of frequencies. This process depends on the properties of the rocks, properties of charges and technology of blasting. It is very important to study how to control vibration induced by blasting in the mitigation of negative effects of blasting in quarries. Maximum values of the particle velocity are depended on great number of different factors. Using the sesmic waves, an optimal millisecond interval has been sought to reduce the intensity of vibrations due to interference of seismic waves. Experiments confirmed the theoretical assumptions that the greatest reduction in vibration intensity occurs when seismic waves are in the opposite phase. The results of the experiments were confirmed in practice during the operation of the blasting works in various quarries in the Slovak Republic.

At blasting operations it is assumed that the method of timing delay calculation is derived from the propagation velocity of seismic waves and their frequency. Furthermore the calculation of the timing delay takes into consideration the effect of disturbance by means of the superposition of seismic waves. Two seismic waves can achieve the maximum disturbance of vibration when the timing delay is the half-period of waves propagation. In the literature (*Duwall and Fogelson, 1962*) the timing delay is stated according to the experience of many projects. Langefors proposed the interval of millisecond timing delay as follows $\Delta t = T/2$ (T is the period of vibration waves), which enables the mutual

* corresponding author, e-mail: blazej.pandula@tuke.sk

interference of the most of vibrations under the condition of the constant vibration cycle and the same vibration types (*Langefors and Kihlström, 1978*). Mogi found out that if the model of linear superposition is applied for the regulate vibration the best result can be achieved if the timing delay error is less than 1–3 ms (*Mogi and Kou, 1999*). The times of delay are assessed both according to the effect of rock medium disintegration and the effect of seismic waves´ superposition. The structural characteristics of the rock medium, in which the blasting operations are carried out, can be identified by means of the measurement of propagation velocity of seismic waves in situ (*Pandula and Kondela, 2010*).

At millisecond timing of blasting operations there can be observed the simultaneous wave propagation from different sources (Fig. 1). If there is a phase difference of two waves in a certain point 2 or another paired multiple, it leads to an interferential amplification If the phase difference is an unpaired multiple, there comes to an interferential attenuation. The different cases of interference are very complicated because the interfering waves can differ from each other in wave length, amplitude, phase and direction of wave propagation. The simplest presence of interference is the one of two wave propagations with the same wave length, spreading through the rock medium with the same phase velocity and the same direction. This is the case of blasting operations (Fig. 2). The final inter-

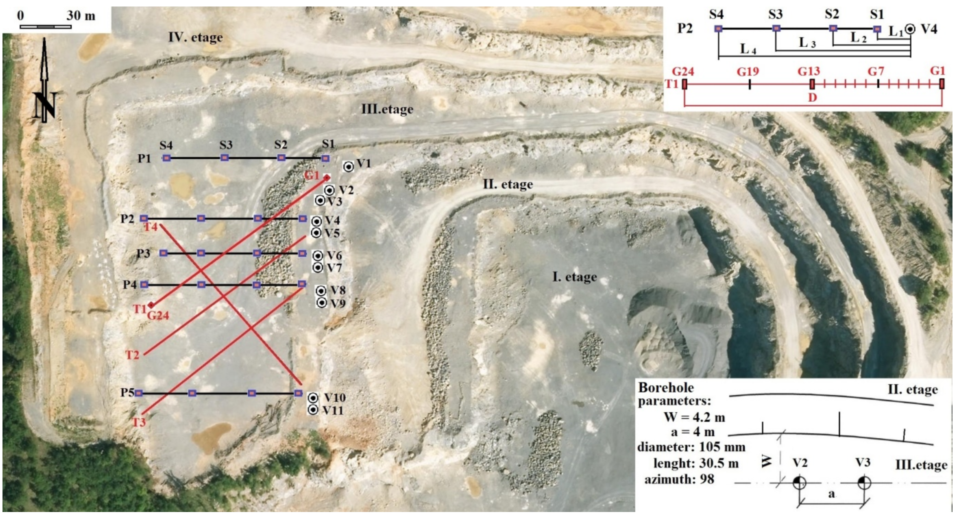

Fig. 1. Position of experimental blasts No. 693 (V1), No. 694 (V2,V3), No. 695 (V4,V5), No. 696 (V6,V7), No. 697 (V8,V9) and No. 698 (V10, V11) in the quarry Trebejov in relation to the measuring profiles P and T. L_1=32,5 m L_2=40 m, L_3=60 m, L_4=80 m. Distance between G1 and G13 = 48 m, between G1 a G24 =96 m.

ference amplitude of two equivalent wave propagations is the highest in the place of seismic waves collision with the same phase and on the contrary the lowest is in the place of seismic waves collision with the opposite phase. Therefore it is necessary to draft the millisecond timing of blasting operations on dependence of structural characteristics of rock medium, which is characterized by the velocity and frequency of seismic waves (*Kou and Rustan, 1992*).

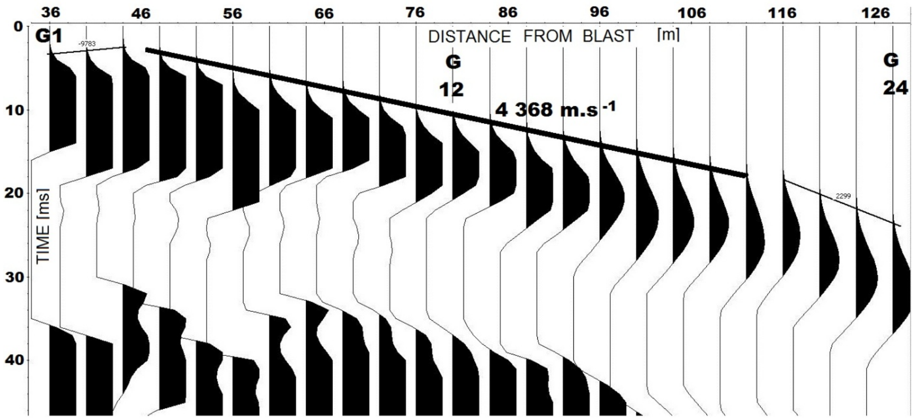

Fig. 2. Seismic record accomplished with measuring apparatus Terraloc Mk 8 of the profile T1 at the measuring standpoint No. 693 with identified propagation velocity of seismic wave 4368 m.s^{-1}, frequency 24 Hz in the rock medium of the dolomites in the quarry Trebejov.

The results of the seismic effects measurements at the experimental blasts, carried out in the quarry Trebejov, proved that the highest attenuation of seismic waves generated by technical seismicity in the quarry Trebejov was achieved at millisecond timing 15 milliseconds and 20 milliseconds. The lowest values of peak particle velocity 0.53 mm.s^{-1} at the surveyed object were recorded at millisecond timing 20 milliseconds. The accurate millisecond timing was enabled due to electronic detonators Unitronic 600.

Key words: seismic waves, experimental blasts, time delay

References

Duwall J. E., Fogelson D. E., 1962: Review of Criteria Estimating Damage to Residences From Blasting Vibrations, U. S. Bureau of Mines RI 5968, 19 pp.

Mogi G., Kou S.-Q., 1999: Optimum delay time design in delay blasting, Sixth international symposium for rock fragmentation by blasting, 145–148.

Kou S.-Q., Rustan A., 1992: Burden related to blasthole diameter in rock blasting. Int. J. Rock Mech. Min. Sci. and Geomech. Abstr., **29**, 6, 543–553.

Langefors U., Kihlström B., 1978: The modern technique of Rock Blasting. A Halsted Press Book., 281–288.

Pandula B., Kondela J., 2010: Methodology of seismic of blastings. SSTVP Banská Bystrica, DEKI Design, s. r. o., p. 156.

Time repeatability of ground radiometric measurements

Andrej MOJZEŠ*

Comenius University in Bratislava, Faculty of Natural Sciences, Department of Engineering Geology, Hydrogeology and Applied Geophysics,
Mlynská dolina, Ilkovičova 6, 842 15 Bratislava 4, Slovak Republic

Abstract: A 450-meters-long line was measured twice by in situ ground gamma-ray spectrometry and soil radon emanometry methods. The first measurement was performed on 31.5.2012 and the second one from 19. to 21.4. 2016, both trying under the similar appropriate weather conditions and at the same stations along the profile with 5–20 m step of measurement. These measurements were a part of complex geophysical measurements carried out for the purposes to characterize the position and some parameters of the Hradište border fault representing the tectonic contact between the Malá Fatra Mts. and the Turiec Basin (Western Carpathians, Slovakia) in the vicinity of the Bystrička Village close to the town of Martin (*Kušnirák et al., 2020*) (Fig. 1). In situ surface gamma-ray spectrometric measurements were carried out using a portable 256-channel gamma-ray spectrometer GS-256 (producer Geofyzika, Czechoslovakia) with 3”×3” NaI (Tl) scintillation detector with determination of total gamma-ray activity eUt [Ur], concentration of ^{40}K [% K], concentration of ^{238}U [ppm eU], and concentration of ^{232}Th [ppm eTh]. In situ soil radon measurements in the form of the volume activity of ^{222}Rn in kBq.m^{-3} were performed on soil air samples taken from approximately 0.8 m depth by a portable radon scintillation (ZnS) detector LUK-3R (producer SMM, Czech Republic). Despite four-years-delay between first and repeated measurements the courses of selected measures show very good visual sameness (Fig. 2). The detailed correlation of all measures between the 2012 and 2016 years is presented in Table 1. The results show the highest linear correlation for thorium concentration (R = 0.87), then for total gamma activity (R = 0.84), volume activity of radon (R = 0.69), potassium concentration (R = 0.66) and the lowest one for uranium concentration (R = 0.12). Very low uranium correlation could be attributed to spectral specification of uranium gamma-ray spectra (wide peak)

* corresponding author, e-mail: andrej.mojzes@uniba.sk

and to its relatively high chemical activity and therefore movement in shallow near-surface horizon.

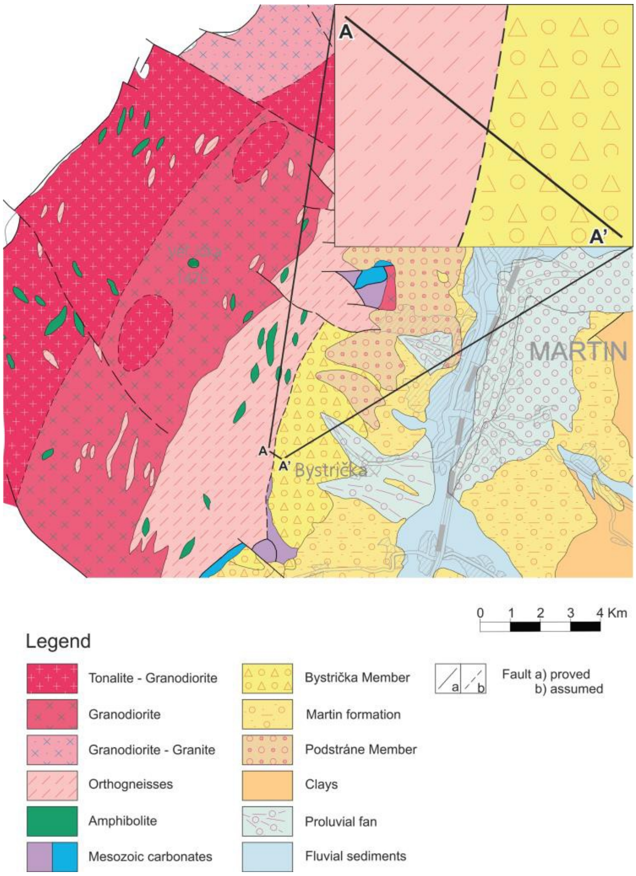

Fig. 1. Location of the investigated Profile A–A’ on a detailed geological map (after *Polák et al., 2008* in *Kušnirák et al., 2020*). Coordinates of the first and final points of the profile are A: 49°03’27.7”N; 18°50’46.57”E and A’: 49°03’19.91” N; 18°51’4.12”E.

On the other hand, the volume activity of ^{222}Rn (^{238}U daughter) in deeper horizon of 0.8 m shows higher stability and therefore relatively high correlation. Very high thorium correlation is typical because of thorium high chemical stability. Generally, the additional uncertainties could be assigned to inaccurate localization of stations and different weather conditions between 2012 and 2016 years. The human activity intervention (e.g. landfill) were not observed.

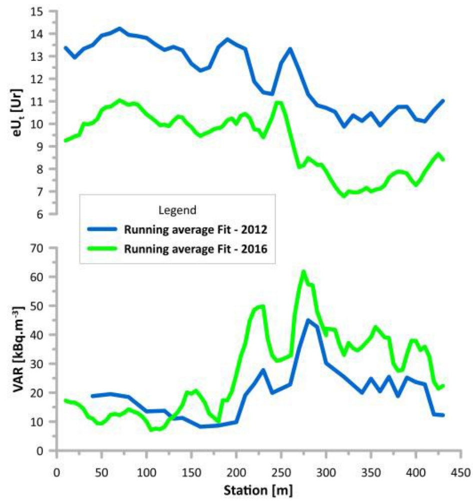

Fig. 2. Example of repeated measurements of volume activity of ^{222}Rn (VAR) and total gamma activity (eU_t) in 2012 and 2016 years.

Table 1. Basic statistical parameters of five radiometric measures in 2012 and 2016 years and their linear correlation (R) 2012 versus 2016.

	2012					2016				
	eU_t	K	U	Th	VAR	eU_t	K	U	Th	VAR
N	45	45	45	45	32	90	90	90	90	89
MIN	9.0	1.2	0.6	5.1	2.9	6.2	0.7	0.2	4.0	4.2
MAX	14.4	2.0	2.8	14.7	63.1	13.4	1.9	2.4	13.0	84.9
AVG	12.2	1.5	2.0	9.8	20.6	9.1	1.2	1.2	8.5	26.9
SD	1.7	0.2	0.5	2.6	12.6	1.5	0.2	0.4	2.6	17.8
R	0.84	0.66	0.12	0.87	0.69	0.84	0.66	0.12	0.87	0.69

Key words: fault, ground gamma-ray spectrometry, soil radon emanometry, weather conditions, repeatability, correlation

Acknowledgement: The contribution was worked out thanks to support of research projects: APVV-16-0146, APVV-21-0159, VEGA 1/0107/23 and VEGA 1/0587/24.

References

Kušnirák D., Zeyen H., Bielik M., Putiška R., Mojzeš A., Brixová B., Pašteka R., Dostál I., Zahorec P., Papčo J., Hók J., Bošanský M., Krajňák M., 2020: Physical properties of Hradište border fault (Turiec Basin, Western Carpathians, Slovakia) inferred by multidisciplinary geophysical approach Geol. Carpath., **71**, 1, 3–13, doi: 10.31577/GeolCarp.71.1.1.

New national realization of the EVRS height system in Slovakia

Miroslava JANČOVIČOVÁ*, Branislav DROŠČÁK, Ján BUBLAVÝ

Geodetic and Cartographic Institute Bratislava,
Chlumeckého 4, 827 45 Bratislava, Slovak Republic

Abstract: Binding geodetic reference systems in Slovakia are defined by the Decree of the Geodesy, Cartography and Cadastre Authority of the Slovak Republic (ÚGKK SR) No. 300/2009 Z.z.. Regarding the height reference systems, two systems are binding: the Baltic Height System after adjustment (Bpv; EPSG: 8357) and the European Vertical Reference System (EVRS). In practice, the most commonly used system in Slovakia is Bpv, although the current realization Bpv57 has been in use since 1957. The reference tide gauge of the Bpv is Kronstadt and the reference heights are normal heights according to Molodensky. Until now, all new levelling measurements are still being incorporated into the original Bpv57 realization. This realization is outdated and shows both global and local inhomogeneity. Keeping high quality heights in Bpv is difficult due to its definition. It uses Krasovsky ellipsoid, S-Gr57 or S-Gr64 gravity system, and the classical method of calculating gravity reduction. On the other side, the EVRS height system is based on geopotential numbers calculated from the latest available data defined by the parameters of the current GRS80 ellipsoid. However, in the realization EVRF2000 defined by the upper mention Decree, the adjustment of the geopotential numbers for all points of the national levelling network (ŠNS) was not carried out. In 2019, current realization of the EVRS system, EVRF2019, was introduced by the BKG Leibzig processing center. A year later, the GKÚ obtained a new, more accurate quasi-geoid model called GMSQ2019 (*Bucha et al., 2019*) for work with EVRS using GNSS methods. GKÚ carried out the adjustment of geopotential numbers on 1st order levelling points in the EVRF2019 realization. Test on the points of the National Spatial Network (ŠPS) showed that the normal heights in the EVRS height system in the EVRF2019 realization, together with the new quasi-geoid model GMSQ2019, would allow the determination of heights anywhere in Slovakia using GNSS methods within an accuracy of 1 to 2 cm. In 2024, the final adjustment of geopotential numbers for all 1st and 2nd order levelling points in

* corresponding author, e-mail: miroslava.jancovicova@skgeodesy.sk

the EVRF2019 realization was performed. The new national realization of EVRS was named Slovak Vertical Reference Frame 2024 with the abbreviation SKVRF2024. It represents a national densification of the EVRS (EVRF2019) official realization. Geopotential numbers for 1st order levelling points were adjusted by connecting to the 7 reference points in the EVRF2019 realization provided by the BKG Leibzig processing center with consideration of their standard deviations. Subsequently, geopotential numbers of the 2nd order levelling points were adjusted by connecting them to the already adjusted 1st order levelling points. This national realization SKVRF2024 was established in Slovakia by the novel of the ÚGKK SR Decree No. 300/2009 Z.z. from the April 1st, 2024. The advantage of the EVRS is that it uses the latest available measurements and a modern approach for the calculation of normal heights using geopotential numbers. The differences between the Bpv57 realization and the national realization SKVRF2024 range from 4 to 18 cm (Fig. 1).

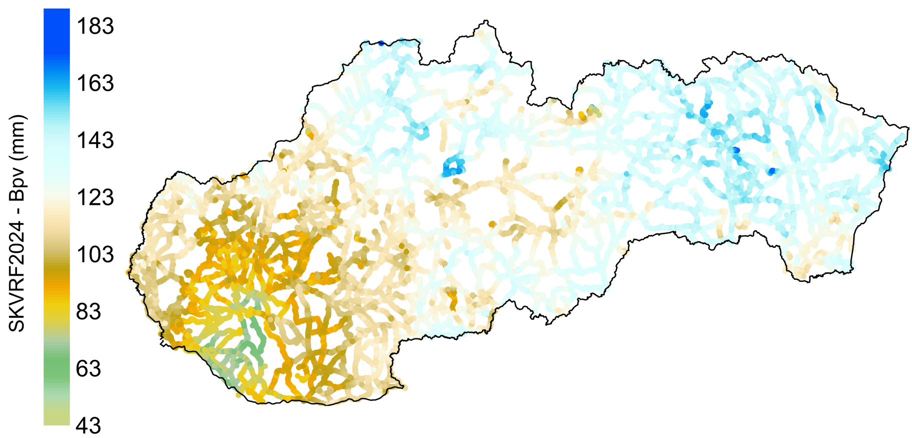

Fig. 1. The differences between the original Bpv57 realization and the national realization SKVRF2024.

Key words: geopotential numbers, quasi-geoid GMSQ2019, national levelling network, EVRS

References

Bucha B., Papčo J., Janák J., 2019: Výskumná analýza kvázigeoidu novej generácie pre územie Slovenskej republiky (Gravimetrický model slovenského kvázigeoidu GMSQ2019). Technická správa. Katedra geodetických základov SvF STU v Bratislave.

Application of the Growth Inversion Approach in volcano gravimetry: detection of thin elongated sources

Jozef BÓDI[1,2,*], Peter VAJDA[1], Antonio G. CAMACHO[3], Juraj PAPČO[4], José FERNÁNDEZ[3]

[1] Earth Science Institute, Slovak Academy of Sciences, Dúbravská Cesta 9, P.O. Box 106, Bratislava, 840 05, Slovakia

[2] Department Engineering Geology, Hydrogeology and Applied Geophysics, Comenius University in Bratislava, Mlynská Dolina, Ilkovičova 6, Bratislava, 842 15, Slovakia

[3] Instituto de Geociencias (CSIC, UCM), C/Doctor Severo Ochoa, 7, 28040, Madrid, Spain

[4] Department Theoretical Geodesy and Geoinformatics, Slovak University of Technology, Radlinského 11, Bratislava, 810 05, Slovakia

Abstract: Observation of gravity changes over volcanically active regions has proved to be useful tool for evaluating hazards associated with volcanic activity. Volcano gravimetry coupled with volcano geodesy can detect underground processes associated with volcanism before they manifest on the surface in the form of eruptions. The discipline provides valuable insights about the invisible (and unreachable) structure of volcanoes and teaches us more about how volcanoes work. It can provide us information about underground mass redistribution in real time, indicating migration of magma or/and hydrothermal fluids.

Spatiotemporal gravity changes observed in field are a complex, composite signal, which first needs to be corrected for atmospheric, tidal, loading, instrumental and hydrological effects. Treatments and discussions regarding such effects can be found in the works of multiple authors, for example *Battaglia et al. (2008)*, *Carbone et al. (2017)*, *Van Camp et al. (2017)* and references therein. However, the correction of the effects mentioned above does not strip the signal of its complexity. The signal is still affected by several contributing factors, such as the gravitational effect of surface and inner deformations, the effect of surface mass changes and effect of internal mass and density changes (for numerical treatment see *Vajda et al., 2019*).

[*] corresponding author, e-mail: geofbodi@savba.sk

The inverse problem, which is one of the options from a variety of gravity data interpretation techniques, poses a great challenge due to its ambiguity and instability. The Growth inversion approach tested here is based on partitioning the subsurface inversion domain into right-rectangular cells and populating the cells with differential densities in an iterative weighted mixed adjustment process, in which the minimization of the data misfit is balanced by forcing the growing subsurface density distribution into compact source bodies (*Camacho et al., 2011*). How the Growth inversion can cope with thin elongated sources is the subject of our study. We use synthetic spatiotemporal gravity changes caused by simulated sources placed in several real volcanic settings. Our case studies demonstrate the benefits and limitations of the Growth inversion as applied to sparse and noisy gravity change data generated by thin elongated sources. Such sources cannot be reproduced by Growth accurately. They are imaged with smaller density contrasts, as much thicker, with exaggerated volume (Fig. 1). Despite this drawback, the Growth inversion can provide useful information on several source parameters even for thin elongated sources, such as the position (including depth), the orientation, the length, and the mass, which is a key factor in volcano gravimetry.

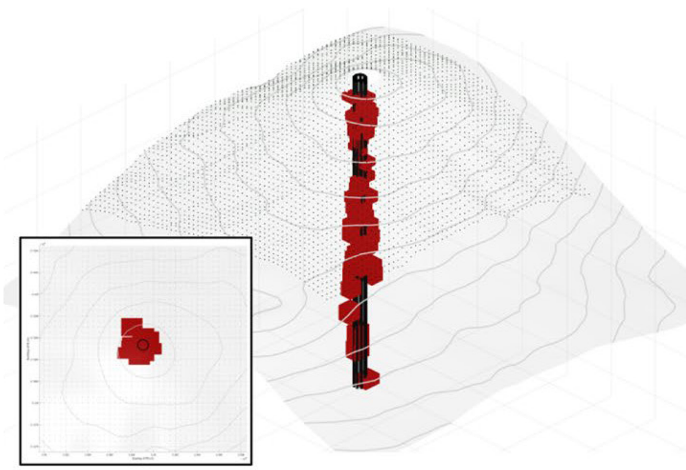

Fig. 1. Growth model (red) reproducing the Teide volcano summit chimney simulated by a thin vertical cylinder (black) of radius 50 m, density contrast 300 kg/m^3 reaching to the depth of 800 m a.s.l.

Key words: gravimetric inverse problem, volcano gravimetry, potential field, synthetic gravity, thin elongated sources

References

Battaglia M., Gottsmann J., Carbone D., Fernández J., 2008: 4D volcano gravimetry. Geophysics, **73**, 6, WA3–WA18, doi: 10.1190/1.2977792.

Camacho A., Fernández J., Gottsmann J., 2011: The 3-D gravity inversion package GROWTH 2.0 and its application to Tenerife Island, Spain. Comput. Geosci., **37**, 4, 621–633, doi: 10.1016/j.cageo.2010.12.003.

Carbone D., Poland P. M., Diament M., Greco F., 2017: The added value of time-variable microgravimetry to the understanding of how volcanoes work. Earth-Sci. Rev., **169**, 146–179, doi: 10.1016/j.earscirev.2017.04.014.

Vajda P., Zahorec P., Bilčík D., Papčo J., 2019: Deformation-Induced Topographic Effects in Interpretation of Spatiotemporal Gravity Changes: Review of Approaches and New Insights. Surv. Geophys., **40**, 1095–1127, doi: 10.1007/s10712-019-09547-7.

Van Camp M., De Viron O., Watlet A., Meurers B., Francis O., Caudron C., 2017: Geophysics from terrestrial time-variable gravity measurements. Rev. Geophys., **55**, 938–992, doi: 10.1002/2017RG000566.

Determining of the depth of limestone bedrock using geophysical methods in Čachtice quarry

Bibiana BRIXOVÁ[1,*], René PUTIŠKA[1], Stanislav JURČÁK[2]

[1] Comenius University Bratislava, Faculty of Natural Sciences, Department of Engineering Geology, Hydrogeology and Applied Geophysics, Slovakia

[2] AEGEO, s. r. o., Karpatské námestie 10A, Bratislava, Slovakia

Abstract: The mining area of the Čachtice quarry is situated in the geomorphological subdivision of the Little Carpathians, part of the Čachtice Carpathians. The mining material of interest is mainly Wetterstein limestone (Middle Triassic) of the Nedzov nappe (core or subsoil of the deposit). Neogene Egenburg sediments, represented mainly by conglomerates, breccias, carbonate sandstones and sandy limestones (a significantly higher clay content when compared to the underlying part of the deposit), form the overlying part of the deposit. Occurring caverns are filled with clay or tectonic clay. Their total amount is estimated at 15%.

It is in the interest of the quarry owners to expand mining in the southern part of the quarry, in the unmined area. The task of geophysics in this part of the quarry was to determine as accurately as possible the depth of the limestone bedrock and the thickness of the overburden material. Geophysical measurements were carried out using seismic refraction tomography (SRT), electrical resistivity tomography (ERT) and ground penetrating radar (GPR).

Using a combination of ERT and SRT it was possible to determine the depth of limestone bedrock and thus the thickness of the overburden material with good accuracy. The methods had good depth range and resolution. However, in a quarry environment it can be difficult to reach the required depth. This is because both methods require straight profiles and the depth range is approximately 1/5 of their length.

The result of the ERT and SRT measurements is an interpreted geological section constructed resulting from the interpretation of the resistivity and velocity profiles (Fig. 1). In the upper part of the resistivity and velocity profiles there are low values indicating the presence of overburden material. At a depth of 5–12 meters there is a significant resistivity/velocity interface corresponding to the onset of limestones.

* corresponding author, e-mail: bibiana.brixova@uniba.sk

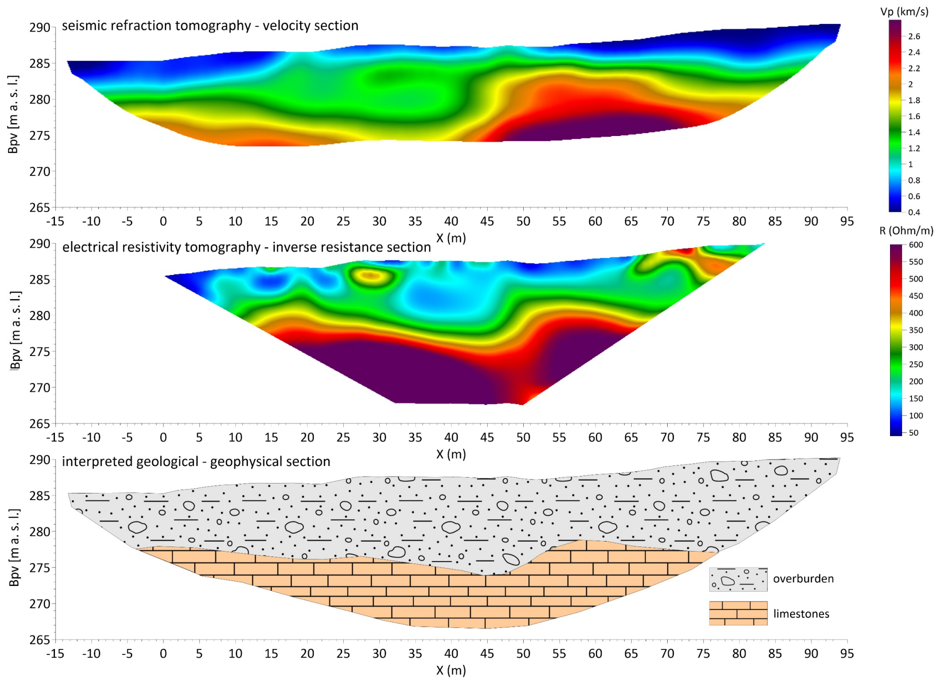

Fig. 1. SRT and ERT measurement results: velocity section, inverse resistance section and interpreted geological – geophysical section.

When interpreting the ERT and SRT measurements, the higher the values of the parameters measured in the limestones, the more compact and higher quality the limestones are. Based on the measured values, we assume that the limestones in the measurement range are fractured. Calibration measurements directly on the surface of limestone mined in the quarry would be required to verify this assumption.

To verify the ability of georadar to locate limestone in the rocky environment of the quarry, GPR measurements were carried out. The MALA GroundExplorer (GX) georadar and HDR (High Dynamic Range) GX antenna with a frequency of 160 MHz were used for this purpose.

In the areas where the limestone comes to the surface, the GPR resolution is very good with a depth range of up to 19 m. In the section where the Quaternary overburden material on the surface is formed by eluvial sediments, deluvial sediments (clays, slope debris) and aeolian sediments (loess, loess clay), the measurement results (Fig. 2) show a significant attenuation. The limestone beneath this overburden cannot be identified.

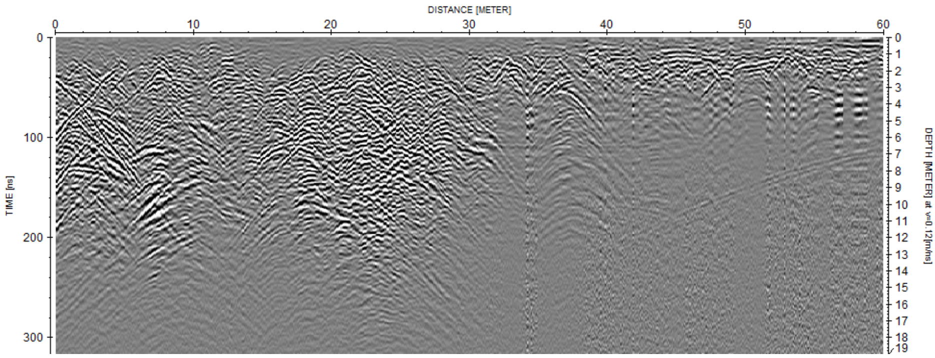

Fig. 2. Results of GPR measurements (radargrams) – profile GPR 28.

At the investigated site of the Čachtice quarry, we had the opportunity to apply and subsequently compare the methods of seismic refraction tomography, electrical resistivity tomography and georadar. After analysing the measured profiles, we evaluated the potential of ERT and SRT to identify the interface between the overburden and the underlying limestone. This interface was not detected by georadar. On the other hand, GPR measurement directly on the limestone block showed very well the quality of the limestone and its tectonic disturbance.

Key words: geophysical measurements, seismic refraction tomography, electrical resistivity tomography, ground penetrating radar, quarry

National gravity network and its modernisation. Vertical gravity baseline.

Branislav DROŠČÁK*, Martin BOROVSKÝ, Adam NOVÁK, Ján BUBLAVÝ, Elena BEŇOVÁ

Geodetic and Cartographic Institute Bratislava,
Chlumeckého 4, 827 45 Bratislava, Slovak Republic

Abstract: The National Gravity Network of Slovakia (ŠGS) in current realisation SGr-95 consist of 294 gravity benchmarks systematically divided into three hierarchical orders (zero order, 1st order and 2nd order ŠGS) based on stability and measuring accuracy. The ŠGS is crucial for all national geodetic and geophysical studies, with each 0-order point's gravity value precisely determined by absolute gravity measurements using instruments such as GABL, JILA G-6, and FG5. In addition, relative gravity measurements have played a significant role in densifying the network and providing essential data for subsequent adjustments and error calculations.

Since 2021, a modernization of the ŠGS has been underway to enhance the precision and reliability of the network. This project focuses on re-measuring the most stable points using state-of-the-art absolute gravimeters, specifically the A10 and FG5X models. The modernization aims to compute the new ŠGS realisation and to achieve a measurement accuracy of better than 5 μGals for new 0-order points using the FG5X gravimeter. Simultaneously, new 1st order points selected from the recent 1st and 2nd order points are being measured with the A10 gravimeter, targeting an estimated accuracy of around 10 μGals. Concurrently, gravity gradients, which serve as a critical link between the measured and stored gravity values at each mark, are being measured and processed.

Another significant achievement in 2024 was the completion of the vertical gravity calibration baseline "Gánovce – Lomnický štít". This baseline enables precise calibration of relative gravimeters across a span of more than 440 mGal difference. Given the line's mountainous terrain, the calibration baseline offers both indoor and outdoor points, allowing year-round operations despite the region's extreme environmental conditions. This has necessitated extended time-lapse gravity analyses and the careful consideration of hydrological factors,

* corresponding author, e-mail: branislav.droscak@skgeodesy.sk

especially given that challenging conditions prevail for almost half of the year. The calibration baseline now includes five base points and eight excentric points, all fully operational and ready for use according to the needs of gravimeter operators. GKÚ and its gravimetric system Laboratory as a part of calibration centre of geodesy will be the operator of the gravimetric baseline.

In summary, the Slovakian National Gravity Network (ŠGS) is not only crucial for national geodetic and geophysical applications but also demonstrates a significant stride towards modernization and precision. The ongoing modernization process, alongside the establishment of the “Gánovce – Lomnický štít” vertical calibration baseline, ensures that the network will continue to serve as a reliable foundation for future research and applications, with improved accuracy and resilience.

Fig. 1. Ballistic gravimeter A10 #20 during a measuring procedure on gravity control point.

Key words: gravity control network, ballistic gravimeter, vertical gravity gradient, vertical calibration baseline

On the distortion of the magnetotelluric response

Alexandra MARSENIĆ*

Earth Science Institute of the SAS,
Dúbravská cesta 9, 840 05 Bratislava, Slovak Republic

Abstract: The presented study deals with the manifestations of magnetotelluric response distortion in two mutually perpendicular polarizations of the electromagnetic field. The cause of the violation of the expected response of the surveyed region is the presence of laterally embedded near-surface conductive inhomogeneity. At the contact of these conductivity-contrasting media, secondary electric fields are generated during the propagation of the original electromagnetic signal in depth. These processes are investigated on a model of a layered half-space in which a near-surface conductive layer is embedded. In relation to the contact surface, we distinguish the polarization of the transverse magnetic mode, in which the electric field is perpendicular to it, and the transverse electric mode, when the electric field is directed along it. Secondary electric fields also have a dual physical nature – Coulombic and inductive. The induction of electric charge at the interface, which has a short-range compensatory effect in the conductive layer with respect to the original electric field, leads to a large-scale secondary field in the resistive medium. Its effect on the response of the transverse magnetic mode is manifested at a distance of several kilometres from the inhomogeneity at practically all frequencies of interest. As a result of the time-varying induction flux from the resistive medium, an electric current is also induced in the conductive layer, which will affect the response of the transverse electric mode. The frequency of the fields plays a multiple role: it determines the bulkiness of the current layer behind the interface, the magnitude of the secondary fields and their attenuation and phase shift when proceeding from the interface. At the same time, it determines the distribution of secondary fields with depth; the transverse magnetic mode disturbances take over the dependence of the primary fields in the conductive layer, while the transverse electric mode disturbances are governed by the dependence of the primary fields in the resistive halfspace. The effects by which the conductive interface extending from the surface to a depth of 1 km contributes to the distortion of the electromagnetic response are shown for three selected frequencies: 0.1 Hz, 1 Hz and 10 Hz.

* corresponding author, e-mail: geofalma@savba.sk

Modelling was carried out using *MATLAB® (2024)* computing software and its add-on product *PDE Toolbox™ (2024)* for solving partial differential equations. The mathematical formulation of this tool is based on a weak (integral) form of partial differential equations, which does not support defining of boundary conditions between subdomains. Therefore, it was necessary to know in advance the behaviour of primary and secondary fields in individual sub- domains and their analytical expressions. These findings were drawn from studies *Marsenić (2020)* and *Marsenić (2024)*. Visualization and understanding of these processes in a simple geometric situation is the first step to creating a realistic model and aims to help the interpretation of measured field data in geologically complex media.

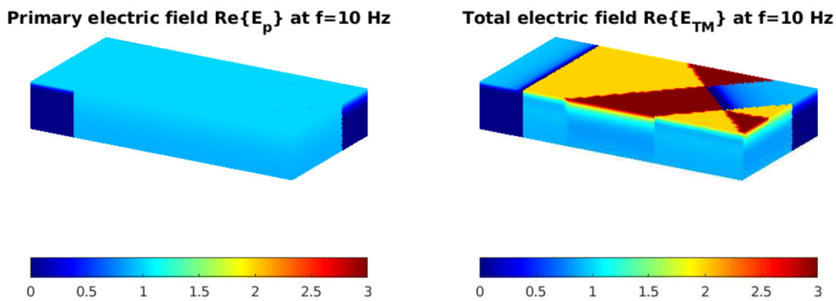

Fig. 1. "Radiation" of conductive inhomogeneities during the penetration of the original electromagnetic signal with a frequency of 10 Hz.

Key words: magnetotelluric response, distortion, charge induction, current induction

References

Marsenić A., 2020: Understanding 1D magnetotelluric apparent resistivity and phase. J. Electromagn. Waves Appl., **34**, 2, 246–258, doi: 10.1080/09205071.2019.1699 452.

Marsenić A., 2024: Physical interpretation of the static shift phenomenon in magnetotelluric data. Appl. Geophys., submitted.

MATLAB®, 2024: MATLAB version: 24.1.0.2603908 (R2024a). The MathWorks Inc., website: https://www.mathworks.com.

PDE Toolbox™, 2024: Partial Differential Equation Toolbox version: 24.1.0.2603908 (R2024a). The MathWorks Inc., website: https://www.mathworks.com.

Detecting underground cavities using seismic ambient noise

Miriam KRISTEKOVÁ[1,2,*], Jozef KRISTEK[1,2], Peter MOCZO[1,2], Martin GÁLIS[1,2]

[1] FMPI Comenius University Bratislava,
Mlynská dolina F1, 842 48 Bratislava, Slovak Republic

[2] Earth Science Institute SAS,
Dúbravská cesta 9, 840 055 Bratislava, Slovak Republic

Abstract: The detection and location of underground cavities is of significant importance in urban development and civil construction, as undetected cavities of natural or artificial origin can pose a considerable geotechnical hazard.

Of particular interest are the underground cavities resulting from underground nuclear explosions. There are a number of reasons for this. One such reason is closely linked to the Comprehensive Nuclear-Test-Ban Treaty (CTBT), an international treaty that prohibits nuclear weapon test explosions and any future nuclear explosions. The detection and location of a cavity generated by an underground nuclear explosion may serve as a useful indicator of an underground nuclear explosion in the context of on-site inspections conducted in accordance with the Comprehensive Nuclear-Test-Ban Treaty (CTBT).

This paper presents two validation cases of a recently developed method for detecting and locating underground cavities. The first case is a CTBT test site near Felsőpetény in Hungary, and the second is a site of the Tiny Tot underground nuclear explosion in Nevada, USA.

We demonstrate that mapping the finite-interval spectral power of seismic ambient noise enables the identification of a location at the free surface above an underground cavity. The method employs single-station measurements at a set of potentially irregularly distributed points in the area on the Earth's free surface over a suspected cavity.

Key words: underground nuclear explosions, seismic ambient noise

[*] corresponding author, e-mail: kristekova@fmph.uniba.sk

GPR measurements for the bridge diagnostics purposes

Michal GRINČ*

INSET s.r.o., organizačná zložka podniku zahraničnej osoby,
Mlynské Nivy 71, 821 05 Bratislava III divízia Žilina, Slovak Republic

Abstract: At present, a great deal of attention, both professional and lay public, is focused on the state of the road infrastructure, on its effective maintenance, with which its repairs are closely related. To effectively invest funds in the maintenance or renewal of the road infrastructure, it is necessary to know the state of the individual elements of this extensive network as best as possible. Recognition of the current state can only be achieved through thorough diagnostics. Perhaps the greatest attention of the professional public in our country is directed to bridges, which are often in inadequate condition. Diagnostics is therefore an extremely important first step to designing effective bridge maintenance solutions. Bridges diagnostic could be divided into three larger units – invasive survey, visual inspection of current faults and non-invasive survey. Each of them has its place, but hopes are mainly placed on progress in the field of non-invasive research. Non-invasive survey is a relatively large group of mostly geophysical methods. The purpose of their use is to collect meaningful data quickly and without damaging the structure under investigation. From this group, ground-penetrating radar survey (GPR) appears to be the most effective survey method. Georadar survey of a bridge object is usually focused on the survey of transition areas with the aim of detecting the presence or the absence of transition plates and their condition. Then, survey of the bridge top is aimed on determining the parameters of the structural layers and analysis of the GPR signal with the aim of determining the places of change in permittivity indicating the possible presence of water in the structure. To calibrate the GPR measurements, the thicknesses of the structural layers determined from the probes into the bridge top are used. Estimation of the actual thickness of the identified layer is currently impossible without the results of the drilling survey. The roadway on the bridge is evaluated qualitatively and its condition is interpreted and anomalies found are commented on, as well as we try to comment on the construction of the bridge. The survey of the bridge top

* corresponding author, e-mail: grinc.michal@inset.com

and transition area is carried out using 3D or 2D ground-penetrating radars. Each profile starts at a sufficient distance in front of the bridge and ends similarly significantly further behind the bridge (min. 15 m). GPR data are processed in the standard manner (*Shaw et al., 2005* and to do that, we are using well known software solution ReflexW (*Sandmeier, 2024*). The results of the GPR road survey are presented usually graphically (Fig. 1). The figure contains processed and interpreted GPR profiles. Areas indicating attenuation of the signal are then marked above the sections and also usually shown on a map. Assuming that the individual structural layers are quasi-homogeneous elements, the received georadar signal can be qualitatively interpreted. With increased attenuation of the signal passing through the structure, the presence of water can be considered as a factor influencing the signal. If there are such anomalies, it can be assumed the long-term presence of water or moisture in the structure.

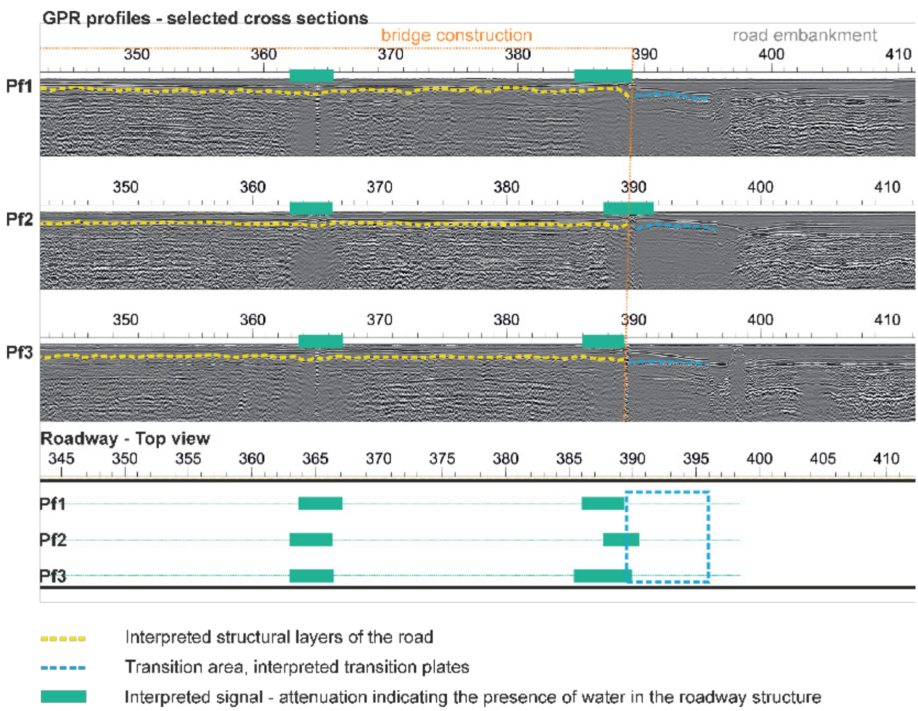

Fig. 1. Example of GPR data interpretation with the legend.

Key words: GPR, bridges, non-invasive diagnostics

References

Shaw M. R., Millard S. G., Molyneaux T. C. K., Taylor M. J., Bungey J. H., 2005: Location of steel reinforcement in concrete using ground penetrating radar and neural networks. NDT & E Int., **38**, 3, 203–212, ISSN 0963-8695, `doi: 10.1016/j.ndteint.2004.06.011`.

Sandmeier K. J., 2024: REFLEXW 32 and 64 bit Version 10.4 User manual, Copyright 1998–2024.

Detecting underground cavities using seismic ambient noise

Martin GÁLIS[1,2,*], Jozef KRISTEK[1,2], Peter MOCZO[1,2], Miriam KRISTEKOVÁ[1,2]

[1] FMPI Comenius University Bratislava,
Mlynská dolina F1, 842 48 Bratislava, Slovak Republic

[2] Earth Science Institute SAS,
Dúbravská cesta 9, 840 055 Bratislava, Slovak Republic

Abstract: The effect of random small-scale heterogeneities in lithosphere and crust has been well recognized for more than a half of century. There is an increasing number of indications that random heterogeneities can play an important role also in modelling earthquake ground motion especially in local surface sedimentary and topographic structures. The problem is being addressed recently in observational and numerical-modeling studies.

We present results of comparison of effects of Random Small-scale Heterogeneities in 1D, 2D and 3D Modeling of Earthquake Ground Motion in two very different macroscopic models – a halfspace and a local sedimentary basin in Colfiorito, Italy.

The main reason for the analysis of results of extensive finite-difference simulations of seismic motion was to look at differences in seismic motions due to reduced dimensionality of the 3D problem. While it is obvious that 3D modeling would be a prime wish and approach, the real practice often restricts numerical-modeling approach to 2D or, even worse, to 1D case due to a variety of reasons, e.g., high computational demands, practical limitations in data and/or knowledge of a local structure.

Our analysis is thus related also to a practical aspect/question in earthquake ground motion analysis and prediction – the possibility to estimate 3D effects of random small-scale heterogeneities based on 2D or even 1D numerical simulations.

Key words: numerical modelling, earthquake ground motion, random small-scale heterogeneities

[*] corresponding author, e-mail: martin.galis@uniba.sk

AdriaArray project

Renata LUKEŠOVÁ[1,*], Lucia FOJTÍKOVÁ[1,2]

[1] Institute of Rock Structure and Mechanics of the Czech Academy of Sciences, v. v. i., V Holešovičkách 94/41, 182 09, Praha 8, Czechia; e-mail: lukesova@irsm.cas.cz

[2] Earth Science Institute, Slovak Academy of Sciences, Dúbravská cesta 9, P.O.Box 106, 840 05 Bratislava Slovak Republic; e-mail: fojtikova@irsm.cas.cz

Abstract: AdriaArray is a multi-national initiative aimed at comprehensively studying the Adriatic Plate and its active margins in the central Mediterranean. This is achieved through a dense regional network of seismic stations (Fig. 1), designed to unravel the causes of ongoing tectonic activity and volcanic formations in the area. Plate-scale observations are enhanced by targeted local and LargeN experiments in critical regions. The AdriaArray project spans from the Massif Central in the west to the Carpathians in the east, and from the Alps in the north to the Calabrian Arc and mainland Greece in the south. The AdriaArray Seismology Group coordinates the deployment of seismic stations and oversees scientific research, ensuring FAIR (Findable, Accessible, Interoperable, and Reusable) and open data sharing. Through seismicity and multi-scale passive seismic imaging analysis, the project aims to establish a foundational understanding of plate deformation processes and the associated geohazards. Details of the project can be found on the Orfeus website: https://orfeus.readthedocs.io/en/latest/adria_array_main.html.

There are several local experiments within the AdriaArray. One of them is the denser network in Romania. This experiment is in charge of IRSM (Institute of Rock Structure and Mechanics of The Czech Academy of Sciences). It consists of densification of the measuring network in the seismoactive area in Vrancea in Romania. The Vrancea seismic zone (VSZ) is located at the sharp bend of the South-Eastern Carpathians in Romania. The character of seismic activity there is rather peculiar since both crustal and subcrustal seismicity are revealed. The crustal seismicity is characterized by low-to-moderate size events spread over a large area with a heterogenous tectonic regime. The subcrustal seismicity is confined to a narrow, almost vertical, cluster of intermediate-depth

* corresponding author, e-mail: lukesova@irsm.cas.cz

earthquakes in the upper mantle with a dominant thrust fault regime (*Radulian et al., 2000, Petrescu et al., 2021*) – see Fig. 2. This seismic nest generates frequent strong earthquakes posing a significant seismic hazard for the densely populated regions of Eastern Europe, despite its remote location from the most active European collisional boundaries. One to five earthquakes with Mw > 7 per century occur here and are felt over a very large territory.

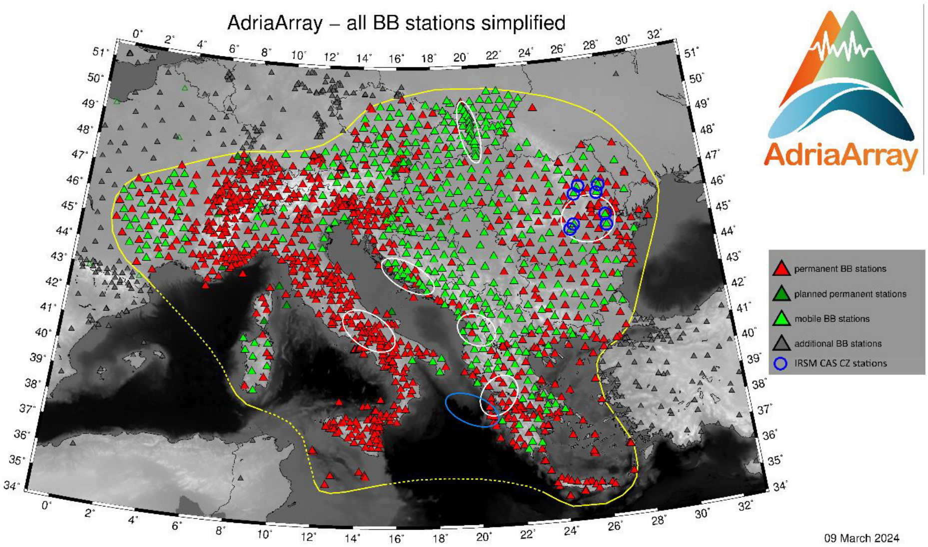

Fig. 1. The distribution of the broadband seismic station within the AdriaArray project. Red triangles represent permanent stations, dark green triangles show planned permanent stations in the region, and light green triangles represent locations of mobile seismic stations operating within the AdriaArray project. Grey triangles are available broadband stations from surrounding regions. The blue circles represent eight seismic stations operated by IRSM CAS CZ. White and blue ellipses represent areas with local experiments (white for land and blue for marine ones). The white ellipse that includes the IRSM stations highlights the local experiment in Vrancea.

Local experiment in Vrancea aims to enhance the seismotectonic model in the Vrancea area using seismic measurements and a careful interpretation of moderate, small, and micro-earthquakes in the region. Their detailed analysis can provide information on their fracturing mode, stress conditions, rotational component and presence of fluids in the focal region.

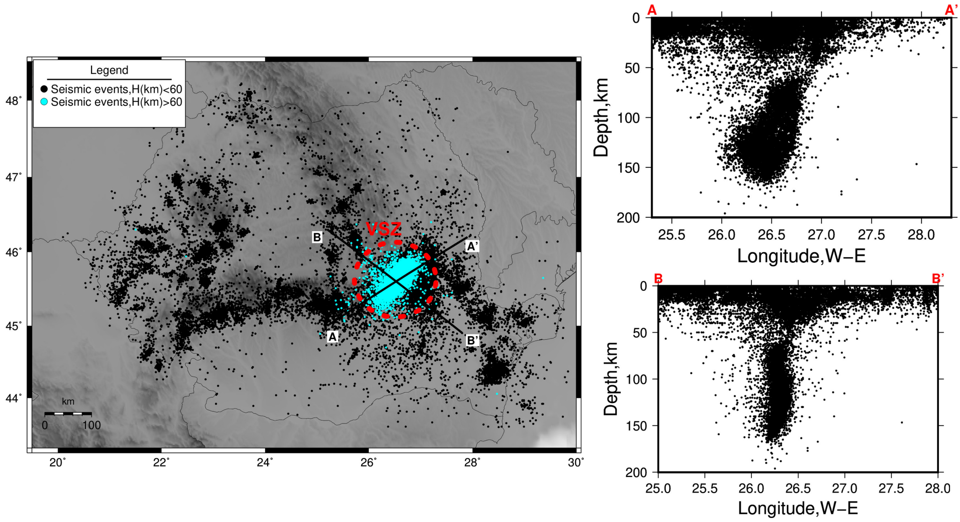

Fig. 2. Earthquake distribution in Romania from the ROMPLUS catalogue (*Popa et al., 2022*) for the period 984/01/01-2023/01/31. The red line represent Vrancea seismic zone (VSZ).

Key words: AdriaArray, seismic experiment, dense seismic network, Vrancea

References

Petrescu L., Borleanu F., Radulian M., Ismail-Zadeh A., Maţenco L., 2021: Tectonic regimes and stress patterns in the Vrancea Seismic Zone: Insights into intermediate-depth earthquake nests in locked collisional settings. Tectonophysics, **799**, 228688, doi: 10.1016/j.tecto.2020.228688.

Popa M., Chircea A., Dinescu R., Neagoe C., Grecu B., 2022: Romanian Earthquake Catalogue (ROMPLUS), Mendeley Data, V1, doi: 10.17632/tdfb4fgghy.1.

Radulian M., Vaccari F., Mândrescu N., Panza G. F., Moldoveanu C. L., 2000: Seismic hazard of Romania: deterministic approach. Pure Appl. Geophys. **157**, 1-2, 221–247, doi: 10.1007/PL00001096.

Higher-order Finite-difference Spatial Operators Across a Material Interface

Jaroslav VALOVCAN[1,*], Peter MOCZO[1,2], Jozef KRISTEK[1,2], Miriam KRISTEKOVÁ[1,2], Martin GALIS[1,2]

[1] FMPI Comenius University Bratislava,
Mlynská dolina F1, 842 48 Bratislava, Slovak Republic

[2] Earth Science Institute SAS,
Dúbravská cesta 9, 840 055 Bratislava, Slovak Republic

Abstract: Recently, we have analyzed consequences of the heterogeneity of the medium, spatial discretization and the Nyquist-wavenumber band limitation for a finite-difference (FD) modeling of seismic wave propagation and earthquake ground motion. We obtained a fundamental restriction for accuracy of numerically-simulated wavefields, and hence for the spatial discretization. The results of our analysis are presented in the triplet of articles by *Moczo et al. (2022)* and *Valovcan et al. (2023, 2024)*. Here, we present results on the application of higher-order FD operators across a material interface. It is obvious that higher-order FD schemes significantly reduce grid dispersion in smoothly and weakly heterogeneous medium. Higher-order schemes involve relatively spatially-long FD operators. Can long FD operators be applied across a material interface? Are the higher-order FD operators more accurate in evaluating spatial derivatives across a material interface? We compare errors of spatial derivatives obtained using the spatial FD operators of the 4th, 6th, 8th, 10th and 12th orders across the material interface for two interface representations. In the first one, a sharp material discontinuity is represented using an exact Heaviside step function. In the second one, the same material discontinuity is represented using a wavenumber band-limited Heaviside step function. Based on the numerical investigations, we formulate implications for the FD modeling of seismic waves and earthquake ground motion in media with material interfaces.

Key words: finite-difference (FD) modeling of seismic wave propagation, higher-order FD operators, material interface, wavenumber band limitation, interface error, fundamental implications from wavenumber-domain analysis

* corresponding author, e-mail: jaroslav.valovcan@fmph.uniba.sk

References

Moczo P., Kristek J., Kristekova M., Valovcan J., Galis M., Gregor D., 2022: Material Interface in the Finite-Difference Modeling: A Fundamental View. Bull. Seismol. Soc. Am., **113**, 1, 281–296, doi: 10.1785/0120220133.

Valovcan J., Moczo P., Kristek J., Galis M., Kristekova M., 2023: Can Higher-Order Finite-Difference Operators Be Applied across a Material Interface? Bull. Seismol. Soc. Am., **113**, 5, 1924–1937, doi: 10.1785/0120230037.

Valovcan J., Moczo P., Kristek J., Galis M., Kristekova M., 2024: How Accurate Numerical Simulation of Seismic Waves in a Heterogeneous Medium Can Be? Bull. Seismol. Soc. Am., **XX**, X, 1–23, doi: 10.1785/0120240049.

Vertical gravity gradient in volcano monitoring – Campi Flegrei study

Pavol ZAHOREC[1,*], Juraj PAPČO[2], Ema NOGOVÁ[1], Roman PAŠTEKA[3]

[1] Earth Science Institute, Slovak Academy of Sciences, Dúbravská cesta 9, Bratislava, Slovak Republic

[2] Department of Theoretical Geodesy and Geoinformatics, Faculty of Civil Engineering, Slovak University of Technology, Radlinského 11, Bratislava, Slovak Republic

[3] Department of Engineering geology, Hydrogeology and Applied Geophysics, Faculty of Natural Sciences, Comenius University, Ilkovičova 6, Mlynská dolina, Bratislava, Slovak Republic

Abstract: Campi Flegrei (CF) belongs to the most hazardous volcanic regions worldwide. The region gained increased attention in the early 1980s, when a pronounced uplift started amounting to 160 cm between 1982 and 1984 centred at Pozzuoli. In May 2024, the CF region was hit by the strongest earthquake swarm in the last decades (maximum magnitude of 4.4).

Gravimetry plays an important role in volcano monitoring. Dynamic processes in volcanic regions produce spatiotemporal gravity changes often accompanied by Earth's surface deformation. Depending on the size of the deformation, gravity changes induced by surface deformation can be significantly higher than those induced by internal density and mass changes caused by internal processes that are the subject of interest. The interpretation often involves correcting observed gravity changes for elevation changes to produce residual gravity changes that can be modelled. The question arises: Which vertical gravity gradient (VGG) should be used, the normal/theoretical (−308.6 μGal/m) or the local (measured)? Views of appropriate type of VGG to use have evolved since the 1980s and vary quite widely across the applications and published studies. The main reason for using measured VGG is to capture the potential contribution of deeper geological sources to VGG, assuming that the topographic component is close to zero. Since the in-situ observed VGG values can significantly differ from the constant theoretical one, particularly in areas of

* corresponding author, e-mail: zahorec@savbb.sk

rugged relief, the situation requires a thorough analysis.

The gravimetric network at CF was established in 1981, and along with gravity monitoring, in situ measurements of the VGG were also conducted. Although the observed point values of VGG at gravity benchmarks were not published, *Berrino et al. (1984)* presented only the average value of −290 µGal/m. We analysed the VGG properties at the CF site in more detail in *Zahorec at al. (2024)*. In the case of the CF caldera, which is often considered as 'reasonably flat area', according to our findings the effect of topography on VGG is usually underestimated, while the effect of deeper geology is overestimated. We model the effect of the near topography on VGG at CF and subsequently verify the results of modelling by in situ observations to support our predictions. The results show that, in terms of VGG, the topographic relief plays a more significant role than the assumed geological sources even at 'flat' calderas such as CF. The often mentioned VGG value of -290 µGal/m does not represent CF area in general. For a better understanding, in addition to CF, we analyse the effect of deeper geological sources on VGG also in the territory of Slovakia using a detailed gravimetric database of Slovakia. As a result, we question the use of in situ observed VGG values when processing and interpreting observed time-lapse gravity changes in volcanic areas accompanied by surface deformation. It is better to use the normal/theoretical value −308.6 µGal/m, where we commit a potentially smaller error. However, these recommendations do not apply to VGG measurements for other purposes (not related to surface deformations), such as mutual comparisons of measurements with different gravity meters (relative or absolute), etc.

Key words: vertical gravity gradient, Campi Flegrei, volcano monitoring

References

Berrino G., Corrado G., Luongo G., Toro B., 1984: Ground deformation and gravity changes accompanying the 1982 Pozzuoli uplift. Bull. Volcanol., **47**, 187–200, doi: 10.1007/BF01961548.

Zahorec P., Papčo J., Nogová E., Pašteka R., 2024: Vertical gravity gradient in volcano monitoring – in situ measured or theoretical? (Campi Flegrei study). J. Volcanol. Geotherm. Res.. Accepted.

Expanded Complete Bouguer Anomaly Map: From AlpArray to AdriaArray

Pavol ZAHOREC[1], Ema NOGOVÁ[1,*], Juraj PAPČO[2], Roman PAŠTEKA[3], Miroslav BIELIK[1,3]

[1] Earth Science Institute, Slovak Academy of Sciences, Dúbravská cesta 9, Bratislava, Slovak Republic

[2] Department of Theoretical Geodesy and Geoinformatics, Faculty of Civil Engineering, Slovak University of Technology, Radlinského 11, Bratislava, Slovak Republic

[3] Department of Engineering Geology, Hydrogeology and Applied Geophysics, Faculty of Natural Sciences, Comenius University, Ilkovičova 6, Mlynská dolina, Bratislava, Slovak Republic

Abstract: Complete Bouguer anomalies are an important tool in the geological interpretation of gravity data. The AlpArray project, covering the Alpine-Carpathian area, introduced a homogeneous map of complete Bouguer anomaly (*Zahorec et al., 2021*). The map was created mainly from terrestrial data from national databases of countries participating in the project. All data were reprocessed and unified (coordinate system and heights), and the formula for complete Bouguer anomaly was taken from *Meurers et al. (2001)*. Additionally, areas without terrestrial data were filled using data from global geopotential models (GGMs). GGMs are mathematical functions that represent the gravity field of Earth or other celestial bodies, and are created from satellite data combined with terrestrial, altimetric, and other gravity data sources. Transformation methods were applied to the final map of complete Bouguer anomalies, and the Modified Horizontal Gradient Amplitude (*Ai et al., 2024*) transformation is presented.

Following the work of the AlpArray initiative, the map of complete Bouguer anomaly was expanded into the so-called AdriaArray area, broadening the region primarily in the southern and southwestern parts. The processing steps from the AlpArray initiative were used, but additional analyses were conducted to determine the most appropriate global geopotential model. While GGMs created from solely satellite data may be sufficient for large-scale research, they do not provide enough detail for more precise studies. The most up-to-date com-

* corresponding author, e-mail: ema.nogova@savba.sk

bined models were examined: EGM2008 (*Pavlis et al., 2012*), EIGEN-6C4 (*Förste et al., 2014*), XGM2019e (*Zingerle et al., 2020*). Data from these various combined GGMs were compared to terrestrial data from the AlpArray database, which is considered the most detailed and accurate representation of reality. The results show that the XGM2019e model smooths the data too much, and a better representation is provided by EIGEN-6C4 combined GGM.

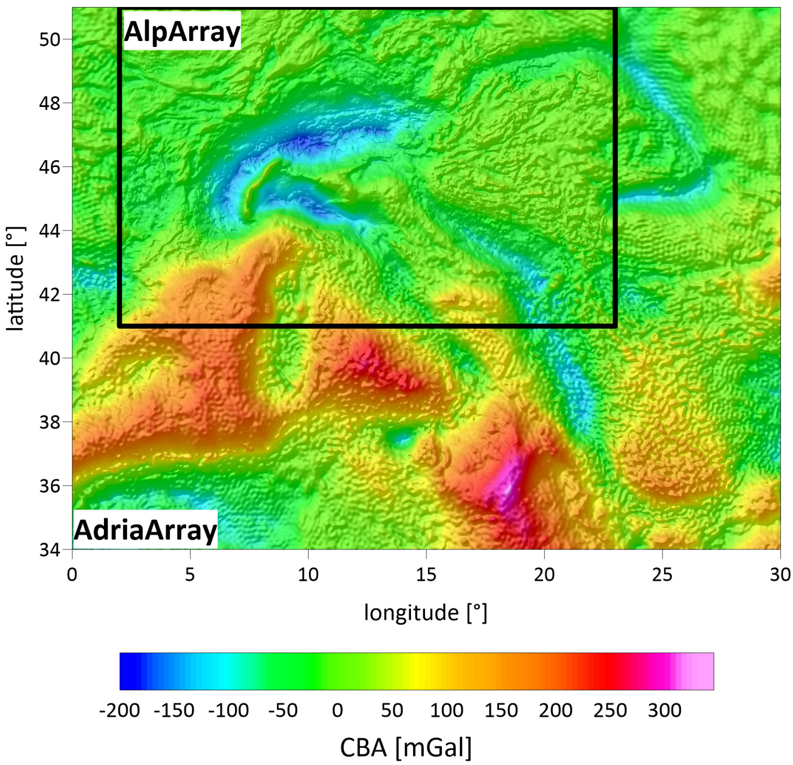

Fig. 1. Map of the complete Bouguer anomaly for the AdriaArray area, compiled from the AlpArray database (mostly terrestrial) and the global model EIGEN-6C4.

The AlpArray and AdriaArray maps were then compiled to create a new complete Bouguer anomaly map for the region between longitudes 0–35° and latitudes 34–51° (Fig. 1). The expansion to the AdriaArray was driven by the 1 authors’ eagerness to extend the map, even though they are not officially part of the AdriaArray project.

Key words: complete Bouguer anomaly, global geopotential models, AlpArray, AdriaArray

References

Ai H., Deniz Totkay H., Alvandi A., Pašteka R., Su K., Liu Q., 2024: Advancing potential field data analysis: the Modifed Horizontal Gradient Amplitude method (MHGA). Contrib. Geophys. Geod., **54**, 2, 119–143, doi: 10.31577/congeo.2024.54.2.1.

Förste C., Bruinsma S. L., Abrykosov O., Lemoine J.-M., Marty J. C., Flechtner F., Balmino G., Barthelmes F., Biancale R., 2014: EIGEN-6C4 The latest combined global gravity field model including GOCE data up to degree and order 2190 of GFZ Potsdam and GRGS Toulouse. doi: 10.5880/icgem.2015.1.

Meurers B., Ruess D., Graf J., 2001: A program system for high precise Bouguer gravity determination. Proc. 8th International Meeting on Alpine Gravimetry, Österreichische Beiträge zu Meteorologie und Geophysik, edited by: Meurers, B., 217–226.

Pavlis N. K., Holmes S. A., Kenyon S. C., Factor J. K., 2012: The development and evaluation of the Earth Gravitational Model 2008 (EGM2008). J. Geophys. Res., Solid Earth, **117**, B4, doi: 10.1029/2011JB008916.

Zahorec P., Papčo J., Pašteka R., Bielik M., Bonvalot S., Braitenberg C., Ebbing J., Gabriel G., Gosar A., Grand A., Götze H.-J., Hetényi G., Holzrichter N., Kissling E., Marti U., Meurers B., Mrlina J., Nogová E., Pastorutti A., Salaun C., Scarponi M., Sebera J., Seoane L., Skiba P., Szűcs E., Varga M., 2021: The first pan-alpine surface-gravity database, a modern compilation that crosses frontiers. Earth Syst. Sci. Data, **13**, 5, 2165–2209, doi: 10.5194/essd-13-2165-2021.

Zingerle P., Pail R., Gruber T., Oikonomidou X., 2020: The combined global gravity field model XGM2019e. J. Geod., **94**, 7, 66, doi: 10.1007/s00190-020-01398-0.

Observation of geomagnetic activity and space weather studies

Miloš REVALLO[1,*], Fridrich VALACH[2]

[1] Earth Science Institute, Slovak Academy of Sciences, Dúbravská cesta 9, 840 05 Bratislava, Slovakia

[2] Geomagnetic Observatory, Earth Science Institute, Slovak Academy of Sciences, Komárňanská 108, 947 01 Hurbanovo, Slovakia

Abstract: Space weather is an important risk factor in today's technolog- ically advanced society. We are currently in the ascending phase of the solar cycle, near the expected maximum, which is responsible for the increase in geomagnetic activity. In this contribution, we deal with the observational and theoretical aspects of geomagnetic activity. We point out the important role of the Hurbanovo Geomagnetic Observatory within the framework of INTERMAGNET network. The mechanisms of strong geomagnetic disturbances are the subject of intensive research today. The classic idea of the ring current as a source of strong magnetic storms is currently being revised, highlighting the role of currents in the auroral oval and the so-called field aligned currents. We studied the local manifestations of disturbances due to intensified auroral oval currents. Another part of our theoretical research concerned modeling and forecasting of geomagnetic activity using the solar wind parameters. We show that a modern approach to the geomagnetic ac- tivity modeling should involve the solar wind-magnetosphere coupling phe- nomena. We also indicate how the geomagnetic disturbances can develop in terms of their solar causes (coronal mass ejections or co-rotating interaction regions). Our recent interest has also been partly oriented towards the analysis of historical geomagnetic data. The aim of this type of research is to obtain longer time series deeper into the past, where it is also possible to identify significant strong magnetic storms. Finally, we will mention the scientific committees SCOSTEP and COSPAR, which provide a framework for space weather research in Slovakia.

Key words: geomagnetic activity, space weather, magnetospheric physics

[*] corresponding author, e-mail: geofmire@savba.sk

2D integrated modelling of the lithosphere and its rheological properties along chosen transects in the Carpathian-Pannonian area

Jana DÉREROVÁ[1,*], Miroslav BIELIK[1,2], Igor KOHÚT[1], Iryna MAKARENKO[3], Olga LEGOSTAEVA[3], Oleksandra SAVCHENKO[3], Vitaly STAROSTENKO[3], Hermann ZEYEN[4]

[1] Earth Science Institute, Slovak Academy of Sciences, Geophysical Division, Department of Gravity and Geodynamics, Dúbravská cesta 9, 840 05 Bratislava, Slovak Republic

[2] Department of Engineering Geology, Hydrogeology and Applied Geophysics, Faculty of Natural Sciences, Comenius University, Ilkovičova 6, Mlynská dolina, Bratislava, Slovak Republic

[3] National Academy of Sciences of Ukraine, Institute of Geophysics by S. I.Subbotin name, Department of Earth's Deep-Seated Processes and Gravimetry

[4] Université Paris-Sud, France

Abstract: Unlike most other methods that focus on interpretation of individual geophysical fields, we utilize 2D integrated modelling approach to determine the lithospheric structure and its rheological properties. The method combines joint interpretation of gravity anomalies, topographic heights, geoidal heights and surface heat flow data. Based on the calculated temperature distribution and assumed rheological parameters of the rocks, we can calculate strength distribution for both brittle and ductile deformation and construct a simple rheological model of the lithosphere.

This method has been used to estimate the lithospheric structure along several transects passing through the Western and Eastern Carpathians and the Pannonian Basin. Previously, a map of lithospheric thickness has been constructed and published. New results, obtained by modelling on different transects, have been added to the map, making it more detailed. The more detailed structures provide a new information that helps to create better understanding of

[*] corresponding author, e-mail: geofjade@savba.sk

geodynamical processes in the Carpathian-Pannonian region.

Key words: 2D integrated modelling, Carpathian-Pannonian region, lithospheric structure

Magnetotelluric interpretation of the contact zone structure between the European platform and the Western Carpathians

Lenka ONDRÁŠOVÁ[1,*], Vladimír BEZÁK[1], Ján VOZÁR[1]

[1] Earth Science Institute of the Slovak Academy of Sciences,
Dúbravská 9, 840 05 Bratislava, Slovak Republic

[2] Department of Engineering Geology, Hydrogeology and Applied Geophysics,
Faculty of Natural Sciences, Comenius University,
Mlynská dolina, Ilkovičova 6, 842 48 Bratislava, Slovak Republic

Abstract: Character of the contact zone between the European Platform and the Western Carpathians has been interpreted in various ways — most often as a collision following the closure of the Northern Penninic Ocean during the Miocene. However, recent magnetotelluric measurements confirm a much more complex situation. For illustration, we have selected several magnetotelluric models crossing this area along profiles, which are located in the northwestern part of Slovakia in Orava and in the eastern part of Slovakia in the Bardejov region, extending into Poland.

The result of the inverse modelling of the collected magnetotelluric data is the distribution of conductivity along the established profiles to a depth dependent on the conductivity of the environment, the frequency of the measured signal and its quality. The final models with depths of 3–8 km were interpreted with regard to previous geological knowledge.

In the deeper structures, clear differences between the western and eastern parts have become evident. While the western section is dominated by the backthrusting of the Flysch Belt over the Klippen Belt, in the eastern section, it is the opposite – the Klippen Belt is thrust over the Flysch Belt, as documented by several authors. The subsequent processes caused, that the southern part of the Klippen Belt is cut off by steep faults, which is also documented in various studies. This contrasting tectonics reflects the different kinematics of the Carpathian block's collision with the European Platform in the western and eastern parts. In the eastern part, after the end of the subduction, frontal thrusts toward the northeast onto the European Platform likely occurred, followed by transpres-

[*] corresponding author, e-mail: geofleon@savba.sk

sional movements along the Klippen Belt. In the western part, subduction was short-lived and limited, with transpressional movements along the European Platform's margin playing a major role. These movements leading to the formation of several shear zones with the northeastern direction and the creation of horsts and grabens, which are not found in the eastern part. In this transpressional period, the fan-shaped structures of the Flysch Belt, as well as the Klippen Belt and other units, have their origins. Although it is possible that the back-thrusting of the Flysch Belt occurred earlier – at the end of the subduction. As the subduction zone migrated southeastward into the Eastern Carpathians, only transtensional movements occurred at the contact between the European Platform and the Western Carpathians, leading to the formation of a deep shear zone. This zone became a channel for the fluid migration from the mantle and the creation of a regional phenomenon – the Carpathian conductivity anomaly.

The tectonic contact of the European Platform and the Western Carpathians is the result of Neogene tectonic development associated with the closing of the North Penninic flysch ocean, its subduction and subsequent collision. As our magnetotelluric models show, today's deep crustal contact is steep and it is the result of an oblique collision and subsequent transtension processes that formed the Carpathian conductivity anomaly.

Key words: magnetotellurics, European platform, Western Carpathians, tectonic contact

Geophysical Study of Crustal Deformation Using Gravity Data: Muzaffarabad and Adjoining Regions in Azad Jammu and Kashmir

Arooj ZULQRANAN[1,*], Michal ŠPRLÁK[1], Muhammad Rustam KHAN[2]

[1] Department of Geomatics, Faculty of Applied Sciences, University of West Bohemia, Pilsen, Czech Republic

[2] bDepartment of Geology, University of Azad Jammu and Kashmir, Azad Kashmir, Pakistan

Abstract: The present research utilizes the Gravity method to investigate Muzaffarabad and its adjacent areas in Azad Jammu and Kashmir. Qualitative interpretation involved creating various maps such as Bouguer Anomaly, Free Air Anomaly, Elevation, Residual Bouguer Anomaly, and Regional Bouguer Anomaly maps. Quantitative interpretation included computing a geological model along the selected profile A-A'. The study revealed subsurface structural features and the thickness of the sedimentary-metasedimentary wedge, identifying two major faults: The Muzaffarabad Fault (MF) and Bagh Basement Fault (BBF). The NW-SE contour trend in the north indicates the MF, while the western part shows the Jhelum strike-slip fault trend. The BBF extends from Mahoter to Shahdara and reaches the Moho depth. The geological model demarcates the MF within the Miocene Murree Formation, dipping at 49° and connecting with a detachment fault. These faults are tectonically active, suggesting a potential for medium to long-duration earthquakes. Numerous active landslides and fault-related folding and faulting highlight the region's seismic activity. Areas above the hanging walls of MF and BBF are unsuitable for heavy civil engineering structures, whereas footwall areas are comparatively feasible.

Key words: gravity anomaly maps, crustal deformation, Muzaffarabad Fault, seismic activity

* corresponding author, e-mail: arojahad@kme.zcu.cz

References

Rustam M. K., Ali M., 1994: Preliminary gravity model of the Western Himalayas in Northern Pakistan. Kashmir J. Geol., 11-12, 59–66.

Rustam M. K., Ali M., 1997: Tectonics of the Hazara and adjoining areas, based on gravity data, Northwest Himalaya, Pakistan. Geol. Bull. Univ. Peshawar, **30**, 273–283.

Utilization of Hg-spectrometry in tectonic line mapping

Vincent KULTAN*

Department of Engineering Geology, Hydrogeology and Applied Geophysics,
Faculty of Natural Sciences, Comenius University,
Mlynská dolina, 842 15 Bratislava, Slovak Republic

Abstract: The HG-spectrometry method is one of the basic geochemical methods. It was included in the complex of geophysical methods for its wide scope already in the 1980s. It is mainly used in ecological and structural-geological research.

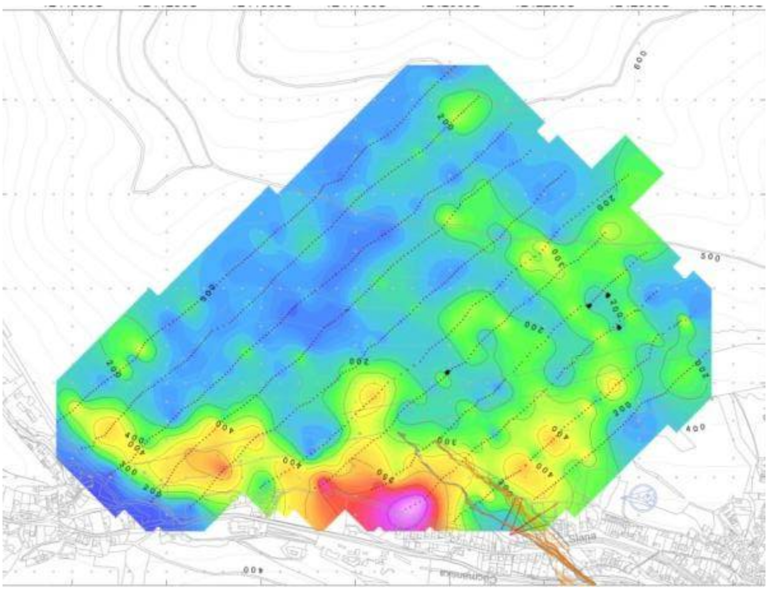

In geological research, the method is used mainly in mapping of tectonic lines and certain types of deposits. Mercury vapors rise along fault lines. There is a measurable Hg anomaly on faults (also unmapped or covered). The Hg anomaly is wider than the existing structure. The size of the anomaly varies

* corresponding author, e-mail: kultan3@uniba.sk

strongly, but the amplitude is always preserved. The Hg measurement describes primarily the tectonic conditions of the monitored area. In specific cases, it is possible to search for bearing structures. The Hg spectrometry method is a fast and economically effective method that enables a quick acquisition of a basic overview of the structural-geological situation of the territory.

Key words: Hg-spectrometry, tectonic faults, mercury vapor

Parameterized Turbulence of the Earth's Outer Core Conditions in Magnetoconvection Models

Jozef BRESTENSKÝ[1,*], Enrico FILIPPI[2], Hari Ponnamma RANI[3], Krishnendu NAYAK[3]

[1] Department of Astronomy, Physics of the Earth, and Meteorology, Faculty of Mathematics, Physics and Informatics, Comenius University, Bratislava, Slovakia

[2] ENEA, Italian National Agency for New Technologies, Energy and Sustainable Economic Development, Rome, Italy

[3] Department of Mathematics, National Institute of Technology Warangal, Telangana, India

Abstract: The turbulence in natural dynamos' regions is frequently parameterized by induction alpha effect and by diffusive beta effect (*Cormier et al., 2022; Rädler, 2000; Roberts and King, 2013; Sokoloff et al., 2014*). In the Earth's core in Geodynamo studies, due to smaller scales of turbulent eddies induction alpha effect is not parameterized, while diffusion beta effect is parameterized by turbulent isotropic (*Brestenský and Filippi, 2024; Roberts and King, 2013*) as well as by turbulent anisotropic magnetic diffusivities (*Brestenský and Filippi, 2024; Filippi and Brestenský, 2020*). In our rotating magneto-convection (RMC) models, the parameterized turbulence with turbulent viscosity, ν, turbulent thermal and magnetic diffusivities, κ and η, respectively, can serve as the basic state convenient for stability study as each physical state (*Brestenský and Filippi, 2024*). This parameterization is suitable, because turbulent eddies formed by basic forces are main transporters of momentum, heat and magnetic field (*Braginsky and Meytlis, 1990; Roberts and King, 2013*).

Linear stability analysis with normal modes in the form of horizontal rolls (*Chandrasekhar, 1961*) is applied on the RMC model of the horizontal fluid planar layer, rotating about its vertical z-axis, and permeated by a horizontal homogeneous magnetic field (*Brestenský and Filippi, 2024; Filippi and Brestenský, 2020; Nayak et al., 2024; Roberts and Jones, 2000; Šoltis and Brestenský, 2010*). In main equations of the RMC models for perturbations to velocity, magnetic field and temperature the diffusive processes are represented

[*] corresponding author, e-mail: brestensky@fmph.uniba.sk

by isotropic or/and anisotropic Laplacians, ∇^2 and $\nabla_\alpha^2 = (1-\alpha)\partial_{zz} + \alpha\nabla^2$, respectively, where α is anisotropic parameter. Different types of modes (*Roberts and Jones, 2000*) (C or O or P) variously inclined to the basic magnetic field (Cross or Oblique or Parallel) arise depending on the input parameters including the α, which is defined as the ratio of isotropic horizontal diffusivity to the vertical one i.e. in full anisotropy, *f*-case, $\alpha = \nu_{xx}/\nu_{zz} = \kappa_{xx}/\kappa_{zz} = \eta_{xx}/\eta_{zz}$. When $\alpha \neq 1$ and $\alpha = 1$, $(\nu\kappa\eta) = (aaa)$ and (iii), respectively, where *i* and *a* denote the isotropic and anisotropic diffusive coefficients, respectively. In the case of partial anisotropy, *p*-case, $(\nu\kappa\eta) = (aai)$ only η is isotropic (*Filippi and Brestenský, 2020; Šoltis and Brestenský, 2010*), i.e. $\eta_{xx}/\eta_{zz} = 1 \neq \alpha = \nu_{xx}/\nu_{zz} = \kappa_{xx}/\kappa_{zz}$. In the pure *h*-case anisotropy, $(\nu\kappa\eta) = (iai)$ only κ is anisotropic, i.e. $\alpha = \kappa_{xx}/\kappa_{zz} \neq 1$ and $\nu_{xx}/\nu_{zz} = \eta_{xx}/\eta_{zz} = 1$.

In marginal stationary (M) and fastest growing unstable modes (F), the modes with maximum growth rate are compared with each other and among four different cases of diffusivities, $(\nu\kappa\eta) = (aaa, aai, iai, iii)$. The studies of M modes were already compared for the cases (*aaa*, *aai*, *iaa*, *iia*, *iai*, *iii*) in (*Filippi and Brestenský, 2020*). All these cases strongly and differently influence the occurrence of convection modes and more significantly for F modes than for M modes; see Figures 1 and 2. Further (*Brestenský and Filippi, 2024*), the F modes contrary to M ones are much better related to all the parameters that are typical for the Earth's outer core (*Aubert, 2020; Cormier et al., 2022; Roberts and King, 2013*), e.g. Rayleigh number, R, Ekman number, E_z, Elsasser number, Λ_z, Prandtl number, p_z, and Roberts number, q_z.

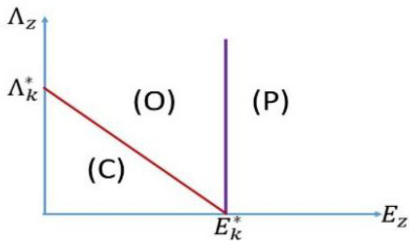

Fig. 1. Λ_z vs E_z is regime diagram in which all C, O, P modes are in their (C), (O), (P) regions, respectively. The points on coordinate axes given by values Λ^* and E^* (Λ^+ and E^+) for M (F) modes determine boundary between (C) and (O) (oblique red curve) regions and between (O) and (P) regions

In Fig. 2 we see that for the parameters, E^+, Λ^+, E^*, Λ^*, for all $\alpha \lesssim 10^3$ and all *f, p, h, i* cases, $E^* >> E^+$ and $\Lambda^* >> \Lambda^+$ does hold, and in particular for $\alpha < 1$. It confirms $E_p^+ = E_f^+ \gtrless E_h^+$ and $\Lambda_h^+ = \Lambda_p^+ \gtrless \Lambda_f^+$ for $\alpha \lesseqgtr 1$, respectively, for the turbulent diffusivity values. Similar results are also observed for molecular diffusivity values. Also, the values of $\Lambda^+$and E^+ for the turbulent diffusivities are greater than the molecular diffusivity values for all *h*, *p* and *f* anisotropy cases.

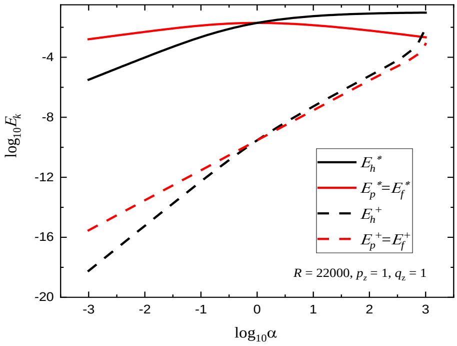

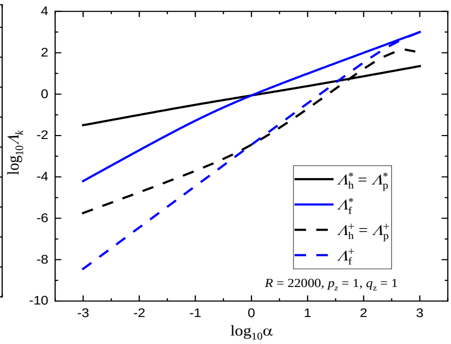

Fig. 2. Regime diagram important parameters E^*, E^+ and Λ^*, Λ^+ vs α for cases *f*, *p*, *h*, *i*, i.e., $(\nu\kappa\eta)$ = (*aaa*, *aai*, *iai*, *iii*), respectively (for turbulent diffusivities at F modes).

Our RMC approach allows to easily deal with very large wave numbers and *R*, and very small *E*, especially in the F modes case, what is usually not possible in the standard geodynamo simulations (*Aubert, 2020; Cormier et al., 2022; Roberts and King, 2013*). In M as well as in F modes, at all the anisotropy cases, the inequality $\alpha < 1$ ($\alpha > 1$) facilitates (inhibits) the convection. The QG balance of forces in the Earth's outer core could prevail in $\alpha \ll 1$ conditions. The MAC balance could be in the uppermost layer of the core with $\alpha \gg 1$ (*Aubert, 2020; Brestenský and Filippi, 2024; Cormier et al., 2022*).

Key words: rotating magnetoconvection (RMC); marginal modes (M); fastest growing modes (F); anisotropic diffusivities (anisotropy); Earth’s core conditions

References

Aubert J., 2020: Recent geomagnetic variations and the force balance in Earth’s core. Geophys. J. Int., **221**, 378–393.

Braginsky S. I., Meytlis V. P., 1990: Local turbulence in the Earth’s core. Geophys. Astrophys. Fluid Dyn., **55**, 2, 71–87.

Brestenský J., Filippi E., 1961: The fastest growing modes in rotating magnetoconvection with anisotropic diffusivities and their links to the Earth’s core conditions. Geophys. Astrophys. Fluid Dyn., **118**, 2, 130–163.

Chandrasekhar S., 1961: Hydrodynamic and Hydromagnetic Stability. Clarendon Press (Oxford).

Cormier V. F., Bergman M. I., Olson P. L., 2022: Earth’s Core: Geophysics of a Planet’s Deepest Interior. Elsevier: Amsterdam.

Filippi E., Brestenský J., 2020: Anisotropic β-effect in the diffusive processes in the rotating magnetoconvection problems. Astron. Nachr., 341, 10, 969–982.

Nayak K., Rani H. P., Rameshwar Y., Jaya Krishna D., 2024: Weakly nonlinear analysis of rotating magnetoconvection with anisotropic thermal diffusivity effect. Phys. Fluids, **36**, 076604.

Rädler K. H., 2000: The generation of cosmic magnetic fields. In: Page D., Hirsch J. G. (Eds.): From the Sun to the Great Attractor; 1999 Guanajuato Lectures on Astrophysics. 556, Springer-Verlag (Berlin), 101–172.

Roberts P. H., Jones C. A., 2000: The onset of magnetoconvection at large Prandtl number in a rotating layer; stationary modes. Geophys. Astrophys. Fluid Dyn., **92**, 3-4), 289–325.

Roberts P. H., King E. M., 2013: On the genesis of the Earth's magnetism. Rep. Prog. Phys., **76**, 9, 096801.

Sokoloff D. D., Stepanov R. A., Frick P. G., 2014: Dynamos: from an astrophysical model to laboratory experiments. Phys. Usp., **57**, 3, 292–311.

Šoltis T., Brestenský J., 2010: Rotating magnetoconvection with anisotropic diffusivities in the Earth's core. Phys. Earth Planet. Inter., **178**, 27–38.

Seismic monitoring in Slovakia and the Oct 9th, 2023 event in Eastern Slovakia

Department of seismology ESI SAS

Earth Science Institute, Slovak Academy of Sciences,
Dúbravská cesta 9, P.O.Box 106, 840 05 Bratislava Slovak Republic;
e-mail: geoflufo@savba.sk

Abstract: Slovakia is a country where moderate seismic activity is observed. Monitoring of seismic activity in Slovakia has a 120-year history. It started in 1901 with the installation of seismograph within the observatory in Stara Dal (Ógyalla in Hungarian, now Hurbanovo), built by M. Konkoly-Thége, the founder of several experimental science disciplines on the territory of present-day Slovakia. Nowadays, seismic activity is monitored by more than 50 seismic stations on the territory of Slovakia.

Considering the statistical data concerning historical, long-term and currently measured and interpreted seismic activity the findings might be summarized as:

– Approximately 70-90 earthquakes with epicentre are recorded annually in Slovakia. These are mostly very weak phenomena that are registered only by seismic stations;
– Every year the inhabitants of Slovakia experience 5 to 6 earthquakes.
– Epicenters of up to a third of these “felt” earthquakes are outside Slovakia, pre-dominantly in Hungary, Austria, Poland and Ukraine. There were felt earthquakes with epicenters as far as in Croatia, Romania and Italy.
– Most of the earthquakes have tectonic origin, some earthquakes have been recorded due to mining or other human activities.

In 2023, exceptionally impactful event occurred: eastern Slovakia was hit by an earthquake with epicentre near village Ďapalovce and local magnitude 5.0 on Oct, 9 at 20:23 local time. This earthquake is the strongest earthquake with epicentre on territory of Slovakia in the last 90 years and the strongest event in the eastern Slovakia in the last 110 years. The seismic waves caused substantial damages to buildings close to epicenter, the epicentral intensity was estimated as 8° of the EMS 98 scale. The focal mechanism shows a reverse fault.

Data from the PACASE-AdriaArray temporary stations were very useful to locate the epicentre, determine the depth of the hypocentre and to calculate the focal mechanism.

ESI SAS received 2566 filled macroseismic questionnaires of which 223 reported damage to buildings. Additional 45 reports were received from the majors of the villages close to the epicenter which helped to more accurately assess damage to buildings and thus determine final macroseismic intensity in these villages.

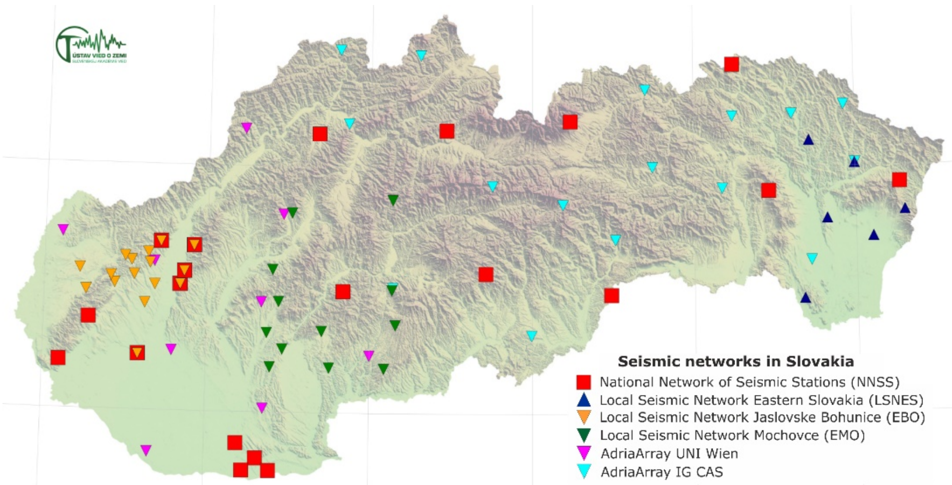

Fig. 1. Seismic stations on the territory of Slovakia.

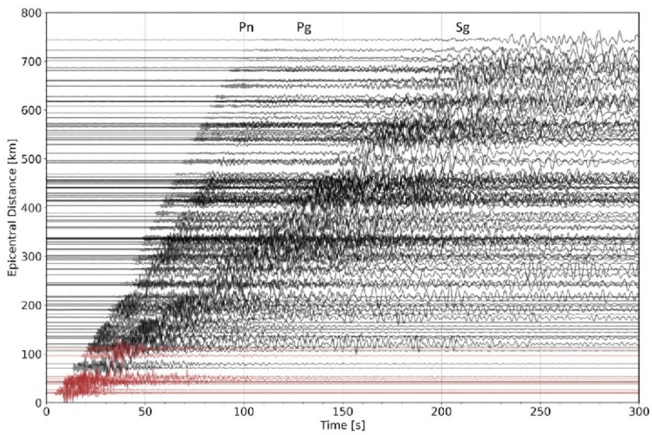

Fig. 2. Seismograms of the event on Oct 9th, 2023, recorded in Europe.

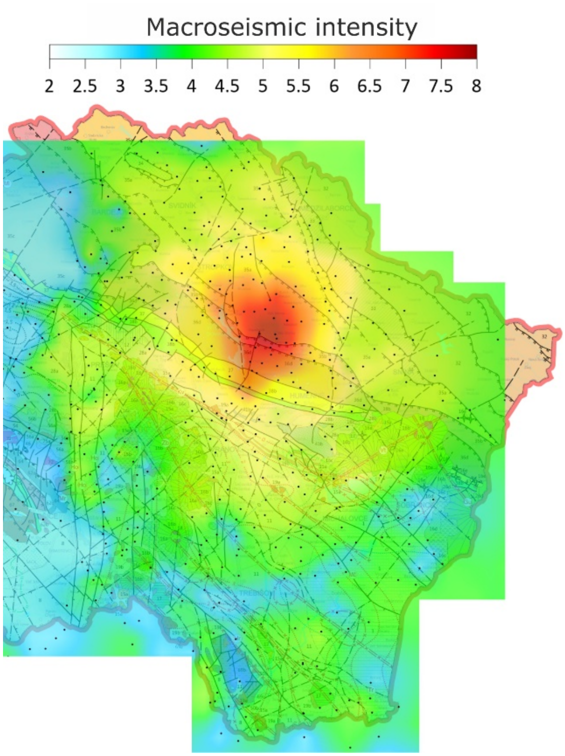

Fig. 3. Macroseismic intensity for the event on Oct 9th, 2023 (on the tectonic map of Slovakia by *Bezák et al. 2004*).

Key words: seismic monitoring in Slovakia, Oct 9th, 2023 Eastern Slovakia earthquake, seismic stations in Slovakia

How historical earthquakes are investigated: case study of Dobrá Voda 1906 and 1930 earthquakes

Róbert KYSEL[1,2,*], Lucia FOJTÍKOVÁ[2], Kristián CSICSAY[2]

[1] FMPI Comenius University Bratislava,
Mlynská dolina F1, 842 48 Bratislava, Slovak Republic

[2] Earth Science Institute SAS,
Dúbravská cesta 9, 840 055 Bratislava, Slovak Republic

Abstract: The territory of Slovakia and Central Europe in general is a region with the moderate seismic activity. There are archeological evidences and contemporary written sources of several historical earthquakes that caused damage of buildings and human fatalities (e.g. 350 Carnuntum earthquake, 1443 Central Slovakia earthquake, 1763, 1783, 1806, 1822 and 1851 Komárno earthquakes, 1600, 1613 and 1858 Žilina earthquakes, sequence of 1778–1779 East Slovakian earthquakes, 1906 and 1930 Dobrá Voda earthquakes, 1885, 1890, 1893, 1914, 1932 and 1941 earthquakes with epicentres near Strážske and Vranov nad Topľou).

In the last decades, only few historical earthquakes with the epicentre on today's territory of Slovakia have been investigated: 1443 Central Slovakian earthquake (*Labák et al. 1996; Varga et al., 2023*), 1763 Komárno earthquake (*Varga et al., 2021*), 1858 Žilina earthquake (*Hammerl et al., 2000*). The lack of systematic and long-term research of historical earthquakes cause major problems by the revision of the catalogue of earthquakes for the territory of Slovakia – the contemporary catalogue is based on more than 70 years old data (!) from Réthly´s 1952 catalogue (*Réthly, 1952*).

Due to the Project New Nuclear Source in Jaslovské Bohunice site, a project on investigation of the 1906 and 1930 Dobrá Voda earthqukes have been realized in 2022–2026 by Earth Science Institute of the Slovak Academy of Sciences in cooperation with Comenius University Bratislava, Faculty of Mathematics, Physics and Informatics. The project is financed and supervised by Jadrová energetická spoločnosť Slovenska, a.s. The project includes collection and analysis of both macroseismical and instrumental earthquake data and the

* corresponding author, e-mail: : robert.kysel@fmph.uniba.sk

determination of new earthquake parameters (epicentral intensities, magnitude, location of hypocentre, focal mechanisms). We present the methodology implemented in the project and the interesting written sources found during the archival research and research of contemporary press.

Key words: historical earthquakes, 1906, 1930, Dobrá Voda

References

Hammerl Ch., Gutdeutsch R., Labák P., 2000: Comparison of three intensity estimations for the January 15, 1858 Žilina (Slovakia) earthquake — Example of importance of the primary source completeness. In: Proc. First Workshop ESC Working Group Historical Seismology, Macerata, Italy, 1–5 September 1999, 44–47.

Labák P., Brouček I., Gutdeutsch R., Hammerl Ch., 1996: The June 5, 1443 Central Slovakia earthquake. ESC XXV General Assembly, Abstracts, Reykjavik, p. 141.

Réthly A., 1952: Earthquakes in the Carpathian basins 455–1918 (in Hungarian). Akademiai Kiadó, Budapest.

Varga P., Győri E., Timár G., 2021: The Most Devastating Earthquake in the Pannonian Basin: 28 June 1763 Komárom. Seismol. Res. Lett., **92**, 2A, 1168–1180, doi: 10.1785/0220200411.

Varga P., Győri E., Fodor C., Timár G., 2023: An Attempt to Determine the Magnitudes and Epicenters of Significant Historical in the Pannonian Basin. Seismol. Res. Lett., **XX**, 1–14. doi: 10.1785/0220220161.